Verification of Satellite Derived Precipitation Estimates over Complex Terrain: A Ground Truth Analysis for Nepal

Ashley Athey

Thesis submitted to the faculty of the Virginia Polytechnic Institute and State University
in partial fulfillment of the requirements for the degree of

Master of Science
In
Geography

Andrew W. Ellis, Committee Chair
David F. Carroll
Robert D. Blevins

May 5, 2015
Blacksburg, VA

Keywords: Nepal, precipitation, satellite derived precipitation

Verification of Satellite Derived Precipitation Estimates over Complex Terrain: A Ground Truth Analysis for Nepal

Ashley Athey

ABSTRACT

Precipitation estimates from the satellite-based Tropical Rainfall Measuring Mission (TRMM) instrumentation play a key role in flood analysis and water resource management across many regions of the world where rain gauge data are sparsely available. Previous studies have produced conflicting results regarding the accuracy of satellite-derived precipitation products, and several authors have called for further examination of their utility, specifically across the Himalaya Mountains region of southern Asia. In this study, daily precipitation estimates generated by TRMM were compared to daily precipitation measurements from a rain gauge network across the country of Nepal. TRMM data were statistically analyzed to quantify their representation of the gauge data during the four precipitation-defined seasons of Nepal. A detailed case study was assembled for the TRMM grid cell characterized by the greatest precipitation gauge density to develop a deeper understanding of local precipitation variability that the coarse resolution TRMM product cannot capture. The results illustrate that TRMM performs relatively well across all seasons, though the performance of TRMM during frozen precipitation events is not clear. In general, TRMM underestimates daily precipitation during the monsoon and pre-monsoon seasons, and overestimates during the winter and post-monsoon season. The case study analysis revealed a threshold for TRMM bias of 10-20mm of daily precipitation, overestimating lighter precipitation events while underestimating heavier precipitation events. Still, TRMM data compare favorably to gauge data, which contributes to the confidence with which they and other satellite-derived data products are used.

Acknowledgements

Thank-you to Dr. Netra Chheri of Arizona State University for providing the Nepalese precipitation gauge dataset. Additionally, I acknowledge Van Smith, Meteorological Connections LLC, and James Clark, National Weather Service, for their assistance with programming and TRMM data collection. I am grateful for the help and support of my thesis committee, David Carroll and Robert Blevins, and advisor, Andrew Ellis.

Table of Contents

List of Figures

List of Tables

List of Abbreviations

APHRODITE	Asian Precipitation Highly-Resolved Observational Data Integration Towards Evaluation
CI	Calibrated Infrared
CMORPH	CPC MORPHing technique
DEM	Digital Elevation Model
DHM	Department of Hydrology and Meteorology
DNA	Data Not Available
FAR	False Alarm Ratio
FBI	Frequency Bias Index
GPM	Global Precipitation Monitor
GPM	Global Precipitation Measurement
IOA	Index of Agreement
MAE	Mean Absolute Error
NASA	National Aeronautics and Space Administration
NST	Nepalese Standard Time
PERSIANN	Precipitation Estimation from Remote Sensing Information using Artificial Neural Network
POD	Probability of Detection
POD	Probability of Detection
PR	Precipitation Radar
RMSE	Root Mean Squared Error
STRM	Shuttle Radar Topographic Mission
TMI	TRMM Microwave Imager
TOVAS	TRMM Online Visualization and Analysis System
TRMM	Tropical Rainfall Measurement Mission
UTC	Coordinated Universal Time
VIRS	Visible Infrared Scanner

CHAPTER 1

Introduction

1.1 Rainfall Variability

Rainfall variability is an important issue within rural mountainous communities globally for an abundance of reasons. This is particularly true within the southern Asian country of Nepal, where the amount of potable water is directly dependent upon the amount of precipitation (Duncan and Biggs 2012), which could be altered under a future, changed climate. According to McDowell, Ford et al. (2013), societies that live in and among the mountainous regions of developing countries are some of the most vulnerable to climate change.

One way to better understand the potential impacts of precipitation variability and change is to analyze historical precipitation events or broader periods of wetness and dryness. Since precipitation gauges are generally not densely distributed across the extreme elevations of countries like Nepal, climatologists must rely on other products, such as satellite-derived estimates, to evaluate precipitation variability and change. Continuous and accurate satellite-derived precipitation data are important for documenting and verifying historical events such as droughts, landslides, and flood events that occur across the rugged terrain of places like the country of Nepal in order to protect life and property. Reliable satellite-derived products are also essential for active climatological monitoring of precipitation, and again, this is especially true across sparsely populated regions of extreme terrain. Accurate measurement of the amount and intensity of precipitation across a region is extremely important for assessing agricultural, geomorphic, and ecological impacts of precipitation events (Barros and Lang 2003).

1.2 Satellite Derived Precipitation Accuracy

To get an accurate account of precipitation in an area, meteorologists and climatologists can use direct measurement from rain gauge networks as well as indirect measurements using satellite-derived precipitation estimates. It is difficult to acquire accurate and spatially representative precipitation measurements at high elevations and across complex terrain due to the difficulty in locating enough instrumentation to capture the high spatial variability in precipitation (Hirpa et al. 2010). Reliable precipitation data across various landscapes are important, as regional precipitation is the main driver of water availability within almost any region.

Although rain gauge data are certainly not without error, they are often taken as "ground truth" and used to validate other methods of estimating the amount of precipitation that fell over a specific region, such as satellite-derived precipitation algorithms. Rainfall is generally inhomogeneous, but the spatial pattern is further influenced by the topography of a region; the more complex the terrain, the more difficult it is to represent the amount of precipitation that fell over an area. For example, the interaction of elevation with low-level atmospheric flow, differential surface heating, and the influence of the rain-shadow effect cause spatial variability in precipitation.

According to Han et al. (2011), rainfall estimates from satellites are more cost-effective and provide a more continuous and consistent data set than ground-based weather stations. Many meteorologists and climate scientists rely on precipitation data derived from the satellite-based Tropical Rainfall Measuring Mission (TRMM) when rain gauge data are unavailable or do not contain the desired measurement density. Such is the case across Nepal, as rain gauges are somewhat sparse across the country. TRMM is one of a number of satellite derived precipitation products available for the region inclusive of Nepal. TRMM data are the focus of the work that follows in this thesis, as Krakauer (2013) found that TRMM data are more accurate across Nepal than other satellite-derived products. A validation assessment of TRMM data over complex terrain would further reveal the value of satellite-derived precipitation estimates in general, and the reliability of the TRMM data specifically.

This thesis presents a validation assessment of TRMM data across the country of Nepal in support of practitioners who could use the information to determine if the data are reliable enough for use in historical water resource, flood, and drought assessments, especially during the hydrologically critical monsoon season. The research uses historical data from precipitation gauges distributed across Nepal to assess the accuracy of TRMM precipitation estimates. Observations from 141 gauges from across Nepal are compared to TRMM satellite-derived precipitation data for a 14-year period to produce statistical characterizations of the historical accuracy of the satellite product. Several other studies have conducted TRMM validation analysis across the Himalayan region, but each suggests that more work is required to make assessments more meaningful. For example, Islam et al. (2010) call for further research using a larger number of rain gage stations, but using similar verification methods as outlined in their research. In answering this charge, a central objective of this research is to quantify the applicability of TRMM data for studying historical precipitation variability and change across Nepal.

1.3 Study Region

The apparent utility of satellite-derived precipitation estimates across Nepal, the complex terrain of the region, and the existing rain gauge network across the region make Nepal ideal for rigorously studying the reliability of satellite precipitation estimates. The southern Asian country of Nepal has some of the most extreme terrain gradients in the world, yet the Nepal Department of Hydrology and Meteorology (DHM) maintains a relatively dense precipitation gauge network. The Himalaya Mountain region of Nepal contains the southern fringe of the Tibetan Plateau (Figure 1), which offers the unique perspective of elevations ranging from 60 meters to over 4,000 meters. The Himalayan mountain range has been of recent interest to meteorologists who aim to study the interaction between precipitation and the landscape. Since elevation in Nepal varies greatly, and since rain gauge networks are difficult to establish at the greatest elevations and within remote areas, the accuracy and availability of satellite-derived precipitation data are extremely important for assessing the rainfall patterns in this area (Yamamoto et al. 2011). The gauge network and the complexity of the terrain make Nepal an excellent

platform for studying the validity of TRMM precipitation estimates over a wide range of elevations.

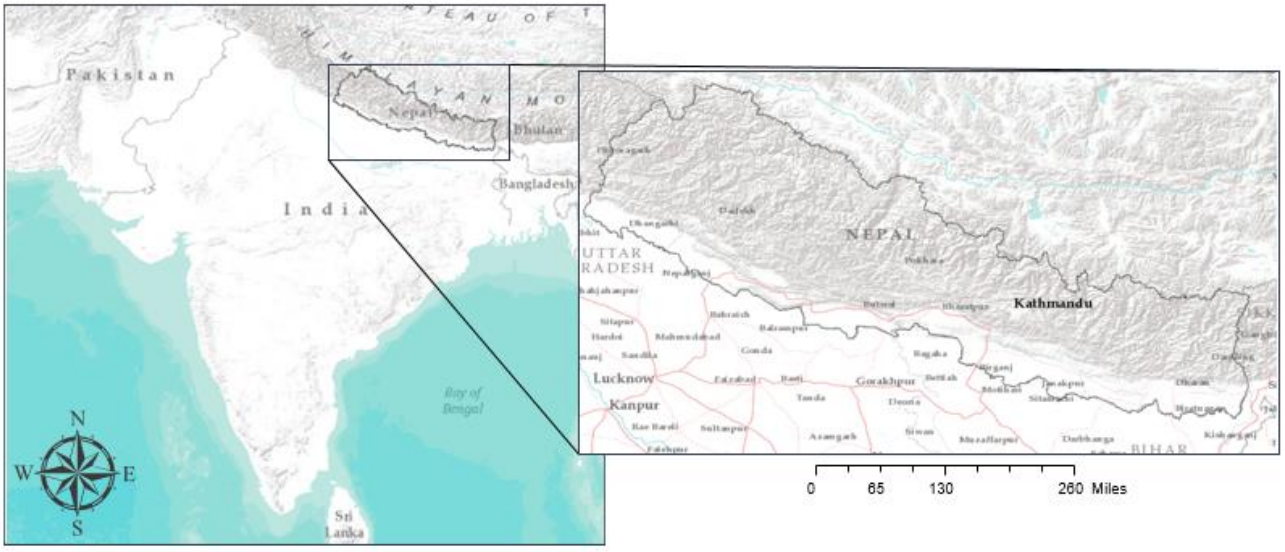

Figure 1. Location of Nepal with elevation shading created with ArcGIS base layers.

Chapter 2

Literature Review

2.1 Use of Precipitation Gauges as Ground Truth

Clearly it is important to have many reliable direct observations when relating precipitation measurements from rain gauges to a gridded precipitation estimation product such as that from TRMM. Numerous studies have previously used rain-gauge measurements as a way to validate satellite derived precipitation (Myrick and Horel 2005; Islam et al. 2010; Han et al. 2000; and Sharma 2007).

The environment in which the precipitation gauges are placed influences their positioning and the accuracy of the measurements. The elevation and terrain across the landscape affects the distribution of precipitation gauges as well as the precipitation patterns themselves. The Department of Hydrology and Meteorology (DHM) of Nepal reports that on average the density of precipitation gauges across the country is about one gauge for every 331 square kilometers, but the density becomes much less in mountainous areas. According to Andermann et al. (2011) and Shresthra et al. (2008), because of the inaccessibility of the gauges at extreme elevations, the majority of the precipitation gauges within the Himalayan Mountains are positioned within valley regions. Not surprisingly, many of the gauges in Nepal are located at low elevations, as it is difficult to monitor and maintain precipitation gauges located in the higher elevations due to rugged terrain and extreme weather conditions. As Barros et al. (2000) found, weather stations at low elevations across central Nepal measured greater rain intensity over shorter time periods when compared to the rain gauges located at higher elevations. This finding indicates differences in precipitation intensity across varying elevations, which will be addressed in this thesis.

Precipitation gauge measurements are subject to systematic and unsystematic errors. Goodison et al. (1981) describes wind as being the most prominent source of systematic error affecting precipitation gauge accuracy. Nespor and Sevruk (1999) also mention evaporation and wetting of the inside gauge walls as potential sources of error in addition to wind. Wind-induced error can be up 10% for rain, and 50% for snow (Sevruk 1985). Of course the errors associated with precipitation gauges depend greatly

on the type of precipitation observing instrument being used, but Yang et al. (1998) indicates that for the bulk of precipitation gauges wind and evaporation have the greatest effect. Monitoring meteorological variables such as humidity and wind remains rare in the Himalaya Mountains region. For example, the Nepal weather stations only record daily precipitation (Uneo et al. 2001).

2.2 Tropical Rainfall Measuring Mission

Remote sensing products, such as the Tropical Rainfall Measuring Mission (TRMM) satellite data generated jointly by the United States' National Aeronautics and Space Administration (NASA) and Japan's Aerospace Exploration Agency (JAXA), are one way for meteorologists to garner estimates of precipitation at relatively fine spatial and temporal scales (Duncan and Biggs 2012). TRMM and other satellite-derived precipitation products can prove extremely helpful when studying historical natural disasters and analyzing precipitation variability in Nepal (Duncan and Biggs 2012). Satellite-derived precipitation estimates are especially helpful when studying the interaction between precipitation and the landscape. However, none of the attributes of satellite data is attractive if the data are not accurate. Previous research has identified factors affecting satellite derived precipitation accuracy, including but not limited to climate, location, landscape, temporal scale, and rainfall type (Barros et al. 2000; Shin et al. 2001; Artan et al. 2007; Sharma et al. 2007; Zhou et al. 2008; Han et al. 2011).

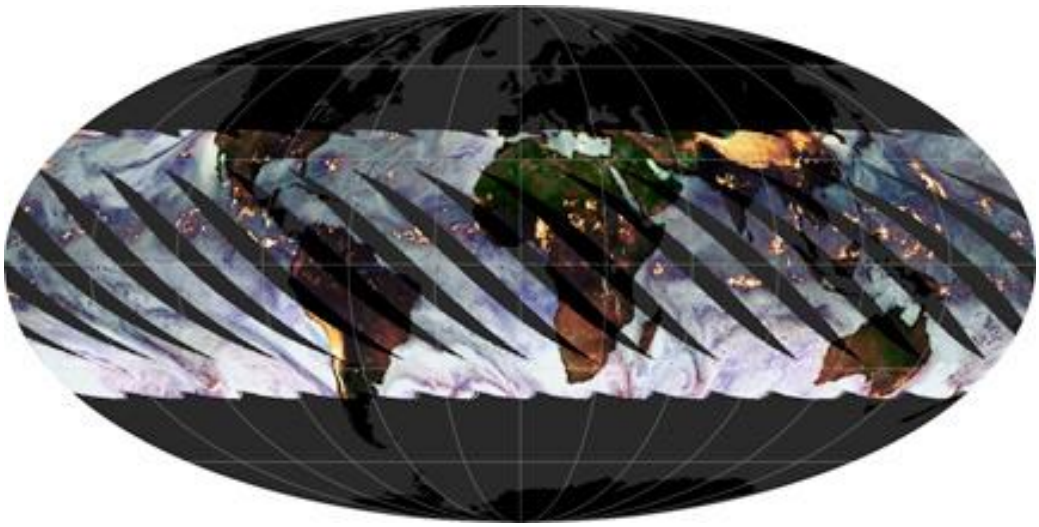

Figure 2. Half of the area for which TRMM makes observations in one day (NASA TRMM Project). The low orbit of TRMM confines its coverage to the tropical regions within 50 degrees latitude of the equator. Source: NASA Earth Observatory - http://earthobservatory.nasa.gov/Features/OrbitsCatalog

The initial purpose of the TRMM program was to monitor tropical and subtropical precipitation (NASA, 2014). Since the launch of TRMM on November 27th 1997, the satellite platform has been collecting various measurements associated with precipitation rate and accumulation over the portion of the globe extending from 50 degrees north to 50 degrees south latitude (Figure 2). The numerous precipitation products produced by TRMM are made possible by the many instruments onboard the satellite.

The TRMM satellite produces numerous rainfall products using the TRMM microwave imager (TMI) and precipitation radar (PR) sensors onboard the satellite (Huffman 2013) (Figure 3). The TMI measures minute quantities of microwave energy emitted from earth and its atmosphere. Analysts working with the raw data are able to calculate estimates of various atmospheric parameters that are associated with the amount of energy received by the microwave imager, including water vapor, cloud water, and rainfall intensity over a wide area (Kummerow et al. 1998). The PR measures precipitation intensity, distribution, and type, and provides three-dimensional maps of storm structure by measuring the 3-dimensional distribution of rainfall over oceans as well as land surfaces ("TRMM" 2014). Kummerow's (1998) report on TRMM satellite data also explains the use of the visible infrared scanner (VIRS), which estimates the altitude of cloud tops. This altitude estimation is made as the VIRS senses the intensity

and spectrum of radiation from the earth-atmosphere system and the infrared wavelengths to calculate cloud top temperature ("TRMM", 2014). The temperature of the cloud top gives an indication of the height of the cloud top, which can be used to estimate the amount of precipitation produced by the cloud following the idea that more vertically developed clouds yield more precipitation (Kummerow et al. 1998). Coverage gaps caused by the orbit of the TRMM satellite are filled with calibrated infrared (CI) data (Huffman 2013). Since each of the sensors carried by the TRMM satellite have different strengths and weaknesses with respect to spatial resolution, swath, and sampling methods, merged rainfall products are produced. Since rainfall is not the only type of precipitation that falls across Nepal (ice and snow occur across the high mountain regions during the winter) investigation of the validity of TRMM during the winter season will be pursued within this thesis.

The TRMM satellite was specifically designed to focus on the tropics, therefore weaknesses in the TRMM estimation arise when trying to assess frozen precipitation amounts (Kummerow et al. 2000). Andermann et al. (2011) describes the accurate estimation of low precipitation amounts, short-lived precipitation events, and frozen precipitation as weaknesses of remotely sensed precipitation products. Andermann et al. conclude that remote sensors cannot accurately determine snowfall, which is the typical type of precipitation across the high Himalaya regions of Nepal (Andermann et al. 2011). It was pointed out by Chen et al. (2013) that the TRMM sensors have limitations when estimating precipitation across landscapes covered in snow or ice. Though Chen et al. (2013) indicate an improvement with TRMM version 7 (V7) over the previous version, when estimating precipitation over high latitude environments.

After more than 17 years of gathering data, the instruments aboard the TRMM satellite were recently disabled. As of July 8, 2014 the TRMM satellite was at the end of its fuel supply and was estimated to be shut down by February 2016. A recent announcement (April 9, 2015) from NASA indicated that the instruments onboard the satellite have been deactivated as of April 8, 2015. TRMM is expected to largely burn-up as it reenters Earth's atmosphere by mid-June 2015. However, the results of this thesis are thought to have utility as a general indicator of the value of other satellite derived products that continue to produce generate data and as guidance to those applying the

historical TRMM data. The error characteristics of the TRMM 3B42 V7, known from here on as TRMM, and the general conclusions of this study will also provide useful feedback to algorithm developers for further improvement of space borne precipitation products and improvement of the new international Global Precipitation Measurement (GPM) satellite mission.

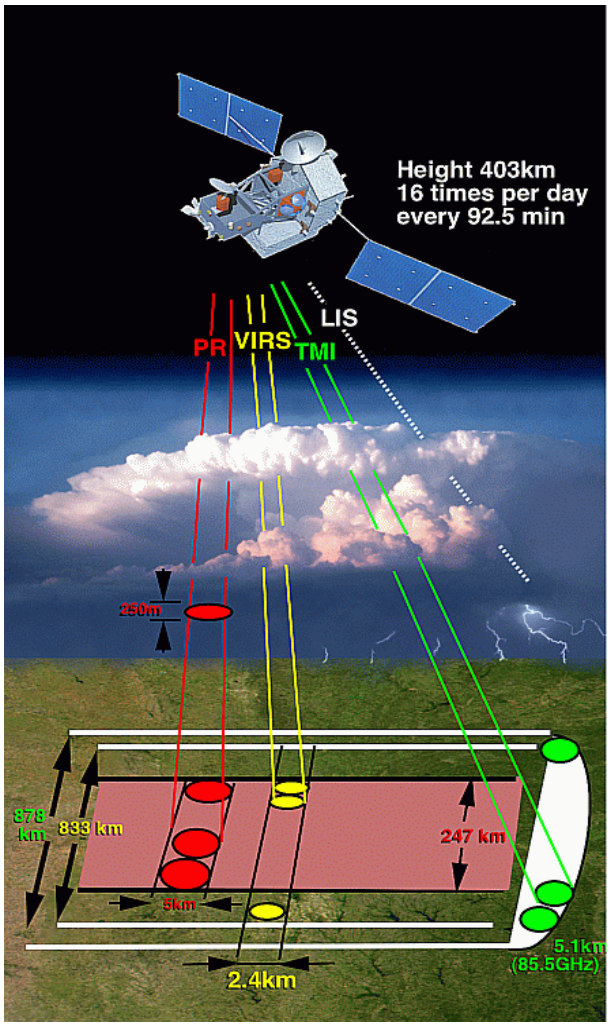

Figure 3. TRMM instrumentation and measurement path diagram as depicted by the NASA TRMM Project. Source: http://trmm.gsfc.nasa.gov/overview_dir/background.html

2.3 Satellite Derived Precipitation Validation

Validation of satellite-derived precipitation estimates over various altitudes and terrain is extremely important for any applications that depend on the spatial and temporal accuracy of the precipitation estimates. Studies have been conducted previously that address the validation of satellite-derived precipitation estimates across various

mountainous regions with similar landscape to Nepal (Barros et al. 2000; Hazarika et al. 2007; Sharma 2007; Dorninger et al. 2008 ; Islam et al. 2010; Han et al. 2011; Duncan and Biggs 2012 and several others). Similarities and differences can be found when comparing the results of these various studies, uncovering gaps and inconsistent conclusions.

Barros et al. (2000) compared TRMM estimates to rain gauge data from the 1999 monsoon season for Nepal and found that TRMM sensors are capable of detecting heavy rainfall in regions of complex terrain with good consistency. Barros et al. also emphasized that if multiple years of satellite data were available, more precise results describing the accuracy of satellite-derived precipitation data could be established, since their study was conducted shortly after the launch of the TRMM satellite. Including a large number of rain gauges over the entire period of available TRMM data would produce a more in-depth analysis of the accuracy of the TRMM satellite precipitation product. Liao and Meneghini (2009) later established that TRMM data estimated precipitation more accurately during light, stratiform-type precipitation events, contrary to the finding of Barros and Joshi et al. (2000).

As stated by Shrestha et al. (2008), research by Sharma (2007) compared TRMM 3B42 estimates with a network of rain gauges in Nepal, but only during the monsoon season. Shrestha et al. also identified that Sharma found that TRMM data slightly overestimated rainfall amounts in the semi-arid regions of Nepal, but underestimated precipitation amounts in humid regions. This study indicates a difference in TRMM accuracy for the various climatic regions of Nepal. While the climatic regions are highly influenced by elevation, terrain also presents a difficulty for satellite derived precipitation products. Dorninger et al. (2008) evaluated various satellite-derived precipitation products across Ethiopia and Zimbabwe and found that in a generally flat landscape the satellite data were more accurate when compared to the estimations over rugged terrain.

The seasonal validation of TRMM, as performed by Hazarika et al. (2007), concluded that TRMM underestimated precipitation during the peak monsoon period, while overestimating precipitation during the dry periods during the year 2004. A drawback to this study is that it focused on only a single year. Their study also found that an increase in the number of stations within a single grid cell used for validation,

decreased the difference between average observed rain and the TRMM estimate. Wang and Wolff (2010) offered an important caveat - that rain gauge measurements cannot be treated directly as "ground truth" data, because rain gauges lack significant area. Because of the extreme differences in the spatial distribution of convective precipitation, it is important to use the rain gauge data as a point data source, and not as an indicator of areal precipitation amounts. It is possible to perform spatial interpolation of rain gauge data by using methods such as distance decay while accounting for elevation differences, but the interpolated data will always be an estimate and driven by the point data.

The accuracy of TRMM data has been addressed by numerous other studies across varying spatial and temporal resolutions. Islam et al. (2010) researched the calibration of the TRMM satellite product over Nepal from the years 1998 through 2007. The validation dataset used in their study was from a rain gauge network that consisted of 15 weather station locations throughout Nepal. The stations were located at elevations ranging from 72 meters to 2300 meters, providing a reasonable range of altitudes to which to compare gauge rainfall measurements to TRMM estimates. The work of Islam et al. (2010) revealed that the TRMM 3B42 data mostly under-represented rain gauge amounts across these 15 stations. However, there is a clear limitation to the robustness of the results due to the small number of stations used.

In another TRMM validation study, Han (2011) found that TRMM data tended to be more accurate during convective rainfall events, when compared to frontal precipitation events across the United States. Han (2011) also noted that rainfall event estimates by TRMM were conservative, as they tended to overestimate minor rain events, while underestimating large rainfall events overall. It is unknown whether this TRMM bias exists in other areas of the world.

Other studies conducted more recently have compared TRMM satellite-derived data with additional sources of precipitation data, from both ground-based networks and other satellite instruments. Research conducted by Duncan and Biggs (2012) compared the satellite-derived precipitation estimates of TRMM 3B42 to a ground-based precipitation data set known as the Asian Precipitation Highly-Resolved Observational Data Integration Towards Evaluation (APHRODITE) of Water Resources project.

APHRODITE is a gridded precipitation product that is based on a relatively large network of rain gauge data throughout Nepal. A caveat with Duncan's study is that the comparison of satellite-derived precipitation data to gridded data formed from interpolation of rain-gauge data is not a direct validation because of the interpolation errors that are inherent in gridded precipitation. This study was conducted for a study period of only 7 years. Duncan and Biggs (2012) concluded that the TRMM precipitation estimates consistently overestimated the amount of precipitation, with the largest error during the monsoon season. Duncan and Biggs' results contradict those of Han (2011), who showed greater TRMM accuracy when considering the convective precipitation of the monsoon period. This study also indicated great disparity between TRMM and Nepalese precipitation gauges during the winter season (Duncan and Biggs (2012). Duncan and Biggs (2012) determined that TRMM estimates are not acceptable and not useful when trying to estimate precipitation across Nepal, contrary to the conclusions of Barros et al. (2000).

In research conducted by Krakauer (2013) multiple satellite-derived precipitation products, including the Climate Prediction Center MORPHing technique (CMORPH) and Precipitation Estimation from Remote Sensing Information using Artificial Neural Network (PERSIANN) were compared using monthly and annual rainfall averages. TRMM data outperformed the other satellite products used in the study area of Nepal, leading Krakauer to conclude that the TRMM precipitation product shows promise for use in water resource applications. Taking the results from Krakauer's study, this thesis will only focus on the validation of the TRMM satellite.

The inconsistency in TRMM validation results calls for further analysis of the satellite derived estimates. The validation work contained in this thesis will address precipitation during all four of Nepal's seasons, and thus it goes beyond the previous research completed by Sharma (2007). A comparison of the TRMM satellite derived precipitation estimates to rain gauge data will be made on a point-by-grid cell basis through this thesis. This approach avoids the interpolation errors inherent in gridded data, contrary to the study completed by Duncan and Biggs (2012) which used interpolated rain-gauge data for TRMM validation. The research by Krakauer (2013) contradicts the conclusion made by Duncan and Biggs (2012), and suggests the need for a deeper

analysis of the verification of TRMM estimates with rain gauge data from across Nepal. The validation research that follows is completed on a considerably longer time period than many of the previous studies of this type in hopes of producing results that are more robust. This thesis answers the call from Hirpa et al. (2010) to perform more validation studies in various stratified mountainous regions in order to discover the limitations of the algorithms used in the satellite-derived precipitation estimates. Ultimately, this thesis research aims to answer the questions and fill the gaps that are evident in the body of literature addressing the validity of satellite-derived precipitation estimates across Nepal and areas that are physically like it.

CHAPTER 3

Climatology of Nepal Precipitation

3.1 Introduction

Precipitation data provided by the Nepalese government for this study were first used to assemble a station-based climatology of precipitation across Nepal. Previous studies have pointed out that precipitation variability over Nepal and Central Asia, especially during the monsoon season, is poorly understood (Shrestha et al. 1999; Ichiyanagi et al. 2007). Therefore, the climatology presented here serves as an important precursor to the verification of satellite-derived precipitation estimates across the region, which is the primary objective of this thesis. The precipitation climatology addresses both the spatial and temporal distributions of precipitation across Nepal, with particular attention paid to the influence of elevation.

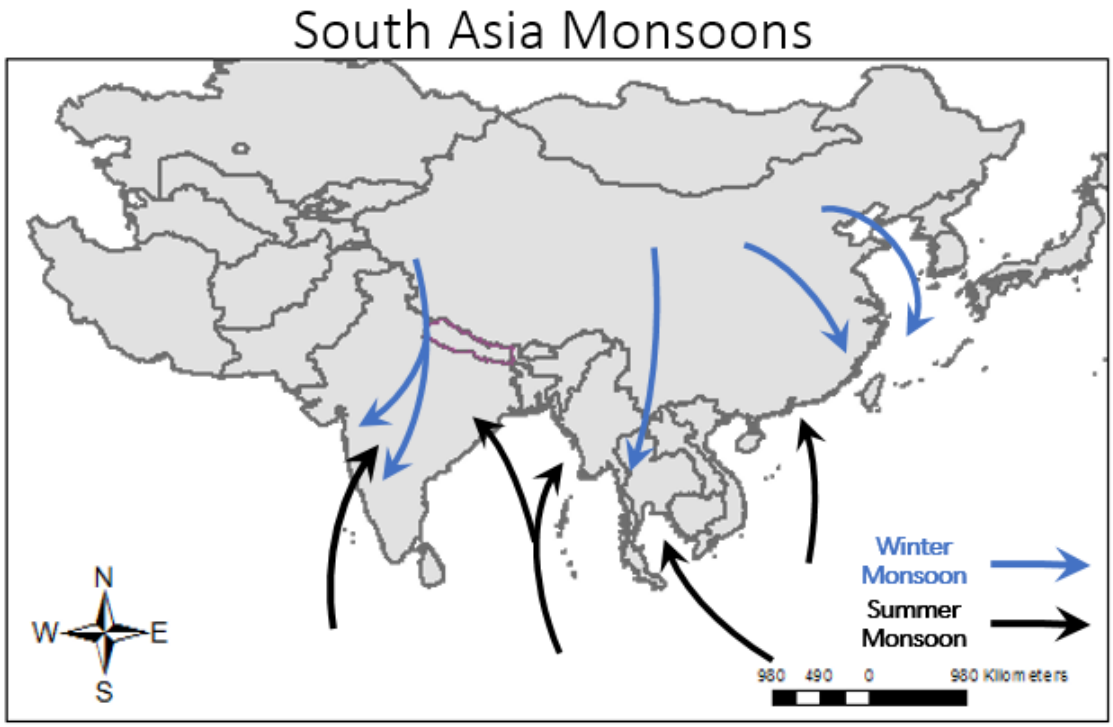

Figure 4. South Asia monsoonal winds patterns – created using ArcGIS basemap layers.

3.2 Background

Previous studies have examined precipitation patterns across Nepal, but the majority of southern Asian precipitation studies exclude the Himalayan region (Kansakar et al. 2004). This climatological analysis goes beyond previous work by Kansakar et al. (2004) and Ichiyanagi et al. (2007) by including a more updated precipitation observation dataset to the year 2011, and by including over 100 additional precipitation gauge observations than Shrestha et al. (2000). Kansakar et al. (2004) called for further research regarding Nepal's spatiotemporal precipitation patterns in support of assessing stress on current and future water resources.

Weather patterns across Nepal vary greatly depending on the season. According to Shrestha and Sada (2013) the four seasons of Nepal include the pre-monsoon (spring), monsoon (summer), post-monsoon (fall), and winter. The Himalaya Mountains act as both a southern barrier to cold air to the north in central Asia during the winter season, and a northern barrier to the moist summer monsoon flow from the south. Kansakar et al. (2004) succinctly characterized the hydroclimatology of Nepal in the following way: a

summer monsoon with later onset and earlier end in the western regions, rainfall increasing largely from north to south in conjunction with east-west oriented mountain regions and a southern moisture source, precipitation in the high northern mountains as a product of westerly large scale weather systems, local rain shadow effects which cause a lack of precipitation and amplified precipitation amounts on the leeward and windward mountain sides respectfully. The drivers of Nepal's spatial precipitation patterns will be taken into consideration throughout this climatological assessment of precipitation.

The atmospheric drivers of Nepal's precipitation patterns differ according to the season, and greatly influence the timing, intensity, and frequency of precipitation. The pre-monsoon season represents the transition from the dry season to the wet season across Nepal. Ichiyanagi et al. (2007) describe a dominant westerly wind during the pre-monsoon as the prevailing pattern shifts from cold northerly winds to the warm southerly winds that accompany the monsoon. The pre-monsoon season is characterized by the majority of precipitation falling during the end of the season, as the maritime influence from the Bay of Bengal begins to strengthen, especially across southeastern Nepal.

Nepal receives 80% to 90% of its annual precipitation during the summer monsoon season (Kansakar et al. 2004), and therefore it is important to understand the processes that typically occur during the monsoon period before any verification analysis is completed. The south Asia monsoon occurs with a seasonal shift in wind direction (i.e., the definition of "monsoon"), and is often evidenced by a change in humidity and precipitation frequency. The south Asia summer monsoon is associated with heavy and frequent rainfall events across Nepal, and these influence the climate of the region greatly. Figure 4 depicts the monsoonal winds during the winter and summer seasons, which profoundly influence precipitation intensity and patterns across the continent. Typically in summer, a moist air mass forms over the Bay of Bengal and propagates westward, bringing a considerable amount of precipitation to Nepal. The synoptic southeastern monsoon flow initiates the majority of the precipitation across the study region (Barros and Lang 2003). Depending on the strength of the convection during the season, the heavy precipitation may reach far northern Nepal across the higher elevations.

The post-monsoon season can be thought of simply as the transition period from the summer monsoon circulation to that of the winter monsoon. The post-monsoon

season begins with the weakening of the summer monsoon influence, from the west to the east. During this season precipitation is largely associated with tropical disturbances, especially across the southeastern regions (Panthi et al. 2015). The majority of Nepal is eventually overtaken by dry, cooler air leading into winter.

The winter monsoon differs from the summer monsoon in several ways. Chang et al. (2006) describe the main differences as being the prevailing wind direction and the amount of moisture inflow during each of the seasons. The winter monsoon is characterized by cold continental winds extending from the north across the high Himalayas, while the summer monsoon season is predicated on winds from the south bringing moist maritime air from the Bay of Bengal (Figure 4). According to Kansakar et al. (2004), Panthi et al. (2015), and Duncan and Biggs (2012) the winter season is generally dry for the majority of Nepal, but occasional large-scale mid-latitude weather systems can bring rain or often snow to the high mountains across northwestern Nepal. The typical snowline occurs from 3,000 to 5,000 meters across the high mountain/high Himalaya regions during the winter, separating the alpine from the temperate climates (Kansakar et al. 2004). According to a previous Nepalese precipitation study conducted by Ichiyanagi et al. (2007) for the time period of 1987 to 1996, the eastern regions of Nepal typically experience greater precipitation amounts across all seasons, except during winter.

Region	Geology and soil	Elevation (masl)	Climate	Average Temp.
Terai	Gently sloping, recently deposited alluvium	200	Humid tropical	> 25^{O}C
Siwaliks	Testing mudstone, siltstone, sandstone. Steep slopes and weakly consolidated bedrock. Tends to promote surface erosion despite thick vegetation	200-1500	Moist subtropical	25^{O}C
Middle Mountains	Phyllite, schists, quartzite, granite, limestone. Stony and course textured soil. Conifer forests commonly found associated with quartzite	1000-2500	Temperate	20^{O}C
High Mountains	Phyllite, schists, quartzite. Soil is generally shallow and resistant to weathering	2200-4000	Cool to sub-alpine	10-15^{O}C
High Himalayas	Limestone and shale. Physical weathering predominates, stony soils	> 4000	Alpine to arctic	< 0 to 5^{O}C

Table 1. Geographic and climate regions of Nepal (Agrawala et al. 2003).

In addition to the regional circulation that yields monsoon season precipitation across the country as a whole, there are steep local terrain features that influence precipitation amounts across small distances. Elevation across Nepal can be used to segregate the country into five main geographic regions with climates ranging from humid tropical to artic across the 200-kilometer stretch of landscape from north to south (Agrawala et al. 2003) (Table 1 and Figure 5). The elevation categories outlined in Table 1 will be used as guidance in the climatological and verification analysis to uncover various topographic patterns in precipitation amounts. Nepal has pronounced geographic diversity with elevations ranging from 59 meters to 8,848 meters, which represents the greatest elevation on earth. The geographic diversity of Nepal gives way to various topography induced precipitation patterns, which will be explored in this chapter.

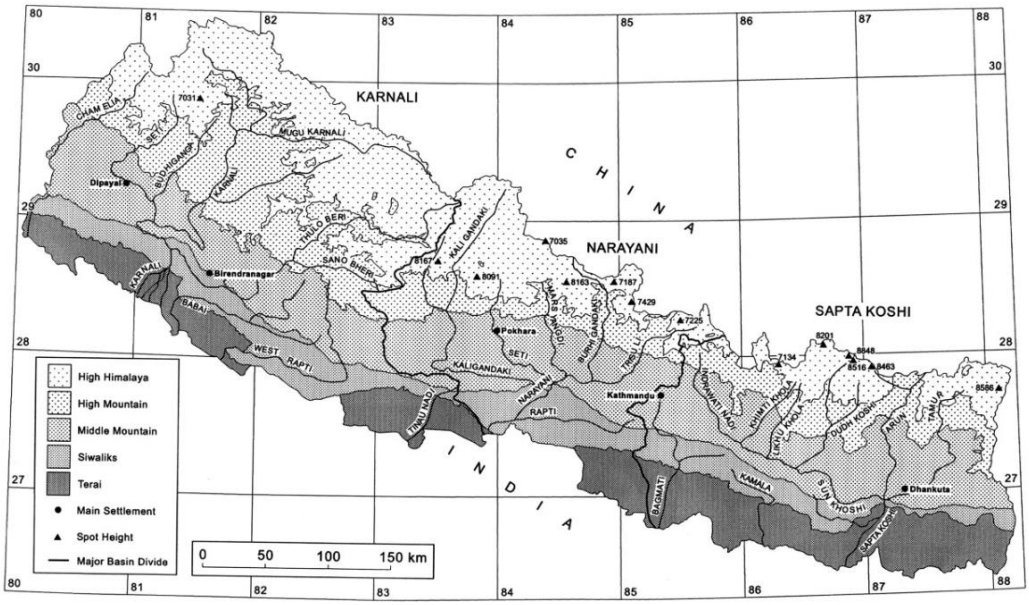

Figure 5. Physiographic regions of Nepal as outlined in Table 1 (Kansakar et al. 2004).

3.3 Methods

To maximize station density and data completeness, and to yield a minimum 30-year climatological period, precipitation data from 210 precipitation stations for the period 1982 to 2011 were taken as a subset of the larger dataset. The climatology offered here goes beyond that of Ichiyanagi et al. (2007) by encompassing 30 years rather than just 10 years. All analyses in this chapter were conducted using only stations with 90% or greater data completeness, as in Ghosh et al. (2009), in order to preserve the quality of the gauge observations. This is compared to the 80% data completeness method used by Ichiyanagi et al. (2007). The following analyses focus on stratifications of the precipitation data at various spatial and temporal resolutions.

3.3.1 Seasonal Analysis

The Nepalese seasons were initially defined using the seasonal dates provided by Dr. Netra Chhetri of Arizona State University (see the "Data" chapter for more information), the source of the gauge precipitation data. These dates were then modified according to the pattern of daily average precipitation through the year (Figure 6a) in order to produce a more detailed definition of each seasonal timeframe. Chhetri's definitions of the seasons across Nepal used the following start dates for each season:

pre-monsoon: March 2nd; monsoon: June 2nd; post-monsoon: October 2nd; winter: December 2nd. Since these dates seem to be rather arbitrary (consistently using the 2nd day of the month in each case), investigation of the mean daily precipitation values (Figure 6a) was conducted to resolve seasonal start dates with a data-driven reasoning. Using Chhetri's start dates as a guide, 30-year mean daily precipitation values were analyzed to identify the greatest difference between consecutive days, with the idea that a large change might be indicative of the mean timing of a seasonal transition. That occurrence near each of Chhetri's start dates was used to determine the start date for each season. As a result, the seasonal start dates to be used in all analyses that follow are: pre-monsoon: March 9th; monsoon: June 4th; post-monsoon: October 4th; winter: December 7th. Each season was individually analyzed for mean precipitation, precipitation frequency, and precipitation intensity patterns as well as precipitation trends.

3.3.2 Mean Precipitation Analysis

To form a basic climatology of precipitation across Nepal, the historical precipitation data for each of the 210 stations were analyzed on various time scales (daily, monthly, seasonal, and yearly). In addition, the mean annual precipitation amounts for each station were analyzed spatially in order to reveal any precipitation patterns evident at that temporal scale across the landscape of Nepal. Next, focus was placed at the seasonal time scale. The period of record mean precipitation across each season for every station was averaged to provide an overview of the spatial variation in seasonal precipitation across Nepal.

3.3.3 Precipitation Frequency and Intensity

Precipitation frequency and daily intensity were evaluated spatially (Figures 8-11) and graphically in order to better understand the data distribution. Seasonal frequency, as calculated as the percentage of days with precipitation, was computed for each of the years in the 30-year period, and then an average of the percentages was calculated for each season. A precipitation day was defined as any day where greater than or equal to 0.01 mm of precipitation was reported in the database for a given station. Frequencies for each station were analyzed and plotted using ArcGIS in order to determine any spatial patterns in precipitation frequency. Next, seasonal values of mean daily intensity were

inspected spatially and temporally for each season. Intensity values were calculated by establishing the sum of precipitation for each station for each year, which was then divided by the number of precipitation days within each year. These annual fractional values were then averaged over the 30-year period to yield a mean precipitation day intensity value (mm/day) for each season.

3.3.4 Trend Analysis

Next, linear regression analysis was performed on the precipitation data over the 30-year period to identify any statistically significant linear trends. In order to test the null hypothesis that no trend is evident in the yearly mean precipitation across each season, the p-value (percent confidence) was calculated for each of the 210 stations across Nepal. The significance level for the first round of regression calculations was set for 0.10 (i.e., 90% confidence) to begin to distill the stations to those that may possess trends in precipitation. Stations with a raw precipitation time series characterized by a strong relationship with time (year) (i.e., a p-value of less than or equal to 0.10) were further analyzed for significance. First the raw data were normalized using the normal scores function of the Minitab statistical software package. This was done to comply with the basic assumption of normality in the data distribution when applying simple linear regression. These data were then subjected to a second linear regression analysis in order to more appropriately test the significance of the time-precipitation relationship. Any time series for which linear regression between the normalized precipitation and time yielded a p-value of less than or equal to 0.05 (i.e., 95% confidence) was considered to be statistically significant. The few time series meeting this criterion were than analyzed visually through plotting to qualitatively determine if the trend was linear, as linear regression suggests, or if the trend was the product of a more suspect step-change in the data. Step changes can certainly be manifestations of true climate variability or change, but often they are systematic changes in non-physical controls, such as instrumentation or observer changes. As such, only time series evidenced by a linear trend were evaluated further. After this final analysis the slope of the regression line for the raw precipitation-time relationships were noted to establish the magnitude of the precipitation change (mm/year). The correlation coefficient (r) representing the co-

variability between each precipitation variable and time (year) was analyzed for each season. A Pearson correlation coefficient was calculated as

$$r = \frac{\sum_i (x_i - x)(y_i - y)}{\sqrt{\sum_i (x_i - x)^2}\sqrt{\sum_i (y_i - y)^2}}$$

and where x represented the annual precipitation value and y represented time (year). Each correlation coefficient value was squared to obtain an approximation of the coefficient of determination (R^2). The R-squared value represents the fraction (or percent) of variance in the precipitation variable that is explained by time.

3.3.5 Elevation Analysis

The extreme elevation changes across Nepal necessitate characterization of precipitation by elevation. The 210 stations used to construct the climatology are located at elevations ranging from 72 to 3,465 meters above sea level. The stations were organized into 500-meter elevation bins based on the elevation noted for each station. This idea was taken from the Nepalese precipitation study conducted by Ichiyanagi et al. (2007), who had a similar count and spread of precipitation gauges. These 500-meter bins were also configured with guidance from the information in Table 1 in order to ensure inclusion of all elevation types. Mean annual precipitation for each of the stations across the 30-year time period within each 500-meter elevation bin was considered, and the standard deviation was calculated for each set of elevation-defined categories. This was done in the spirit of revealing simple elevation-driven differences in precipitation historically.

3.4 Results

Mean daily precipitation (Figure 6a) calculated from all 210 precipitation gauges represents the average amount of precipitation that fell at a station location on each day of the year over the 30-year climatological period. There are distinct wet and dry periods across Nepal, with the wettest and driest days of the year being July 10th and December 6^{th,} respectively. As a whole the mean daily precipitation amounts tend to follow a bell-shaped curve, with the majority of the precipitation falling during the period July through August, with significantly less precipitation observed on average during November and December. The seasonal distinctions appear to be sensible according to Figure 6a,

though the start of the winter and pre-monsoon seasons seem to be less obvious than the monsoon and post-monsoon seasonal start dates.

3.4.1 Mean Precipitation

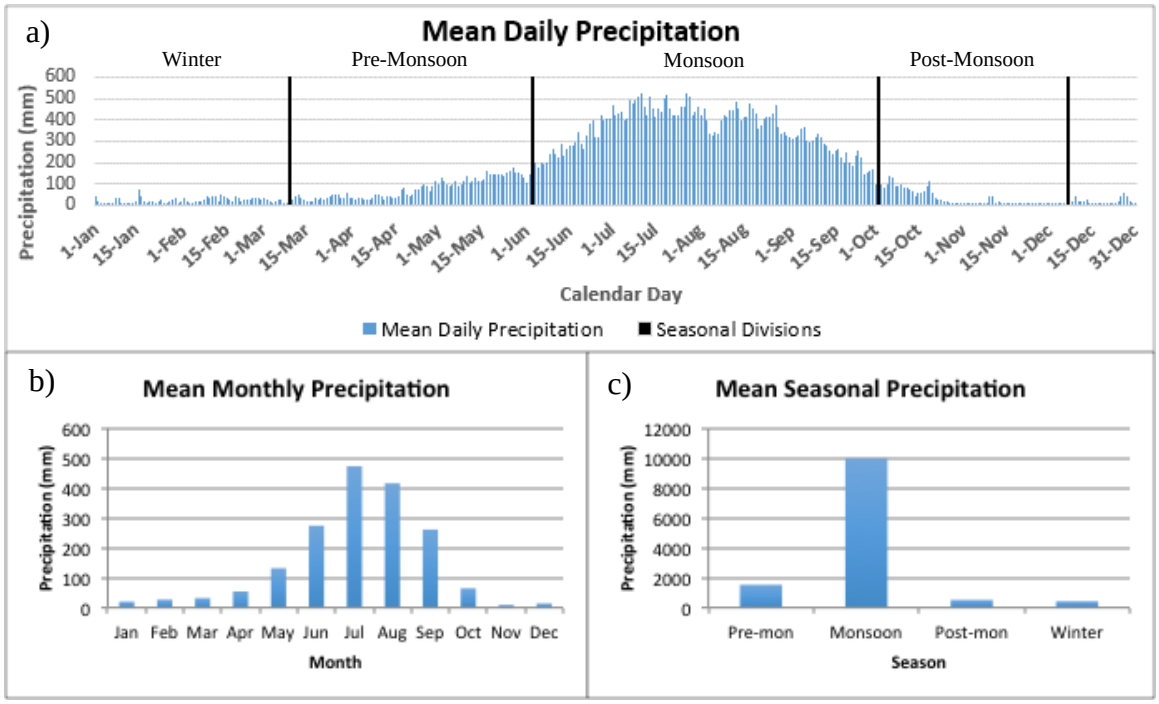

Figure 6. Daily (a), monthly (b), and seasonal (c) mean precipitation from 210 precipitation gauges across Nepal (1982 - 2011). The mean daily precipitation graph also delineates the start of each season used in this verification analysis.

Mean monthly precipitation data (Figure 6b) illustrate a more generalized pattern of precipitation across Nepal through the year than do the daily data. The months transitioning from the post-monsoon to winter season, namely November, December, and January, are characterized by less than 50 millimeters of precipitation. The wettest month across Nepal is July, with an average monthly station precipitation of 473 millimeters, while the driest month is November with 9 millimeters. This monthly depiction offers a broader perspective of the occurrences of the wet and dry seasons, but a more detailed exploration of seasonal precipitation is needed.

Mean seasonal precipitation (Figure 6c) values reveal that the wettest period is clearly the monsoon season, while the driest period defines the winter season. The fraction of annual precipitation across Nepal for each season reveals that on average the country receives 81% of its precipitation during the monsoon season, 12% during the pre-

monsoon season, and 4% and 3% during the post-monsoon and winter seasons respectively.

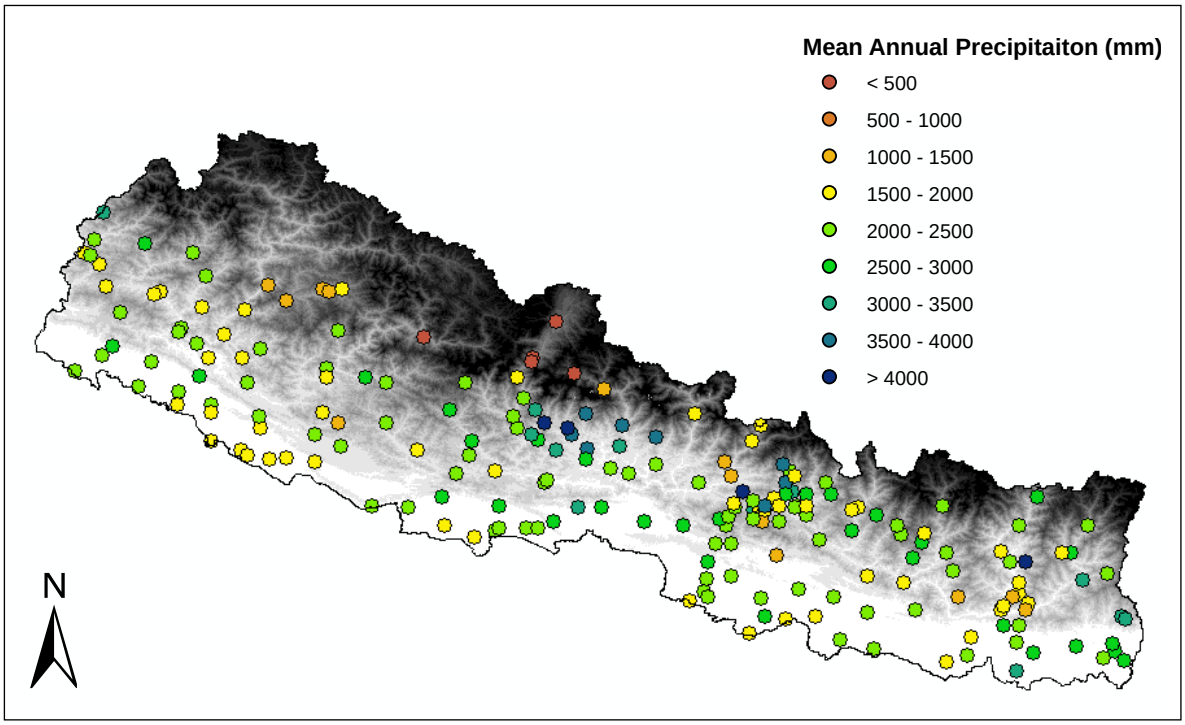

Figure 7. Mean annual precipitation (1982-2011) for each of the 210 precipitation stations, with SRTM DEM base layer.

Mean annual gauge precipitation values were plotted using ArcGIS in order to illustrate the spatial patterns (Figure 7). The few stations with less than 500 millimeters of precipitation annually are all located at higher elevations in the central-northern region of Nepal. Annual precipitation greater than 3500 mm tends to be located across the central regions where elevations are around 2500 meters. Greater annual precipitation amounts are also indicated across the far eastern portion of Nepal. These eastern regions of Nepal are the first (last) to experience the beginning (end) of the summer monsoon precipitation, which could be why more precipitation is observed at these stations. The lesser mean annual precipitation reported by the stations across the west and far northern regions could be from a shorter and less intense monsoon season (Kansakar et al. 2004). The gauges indicating the least amount of precipitation are all located above 2,000 meters in the central northern mountains of Nepal. This clustering of low precipitation gauges indicates a limit to the northern impact of precipitation, as stated previously by Kansakar

et al. (2004). Across the lower elevations to the south, annual precipitation varies between 1500mm and 2500mm, exhibiting more precipitation than the greatest elevations, but less than the mid-range elevations. This pattern may be because the lower elevations across southern Nepal have the benefit of southern moisture, but lack substantial terrain influences, while those a bit farther north have the benefit of both moisture and elevation.

3.4.2 Winter Season Analysis

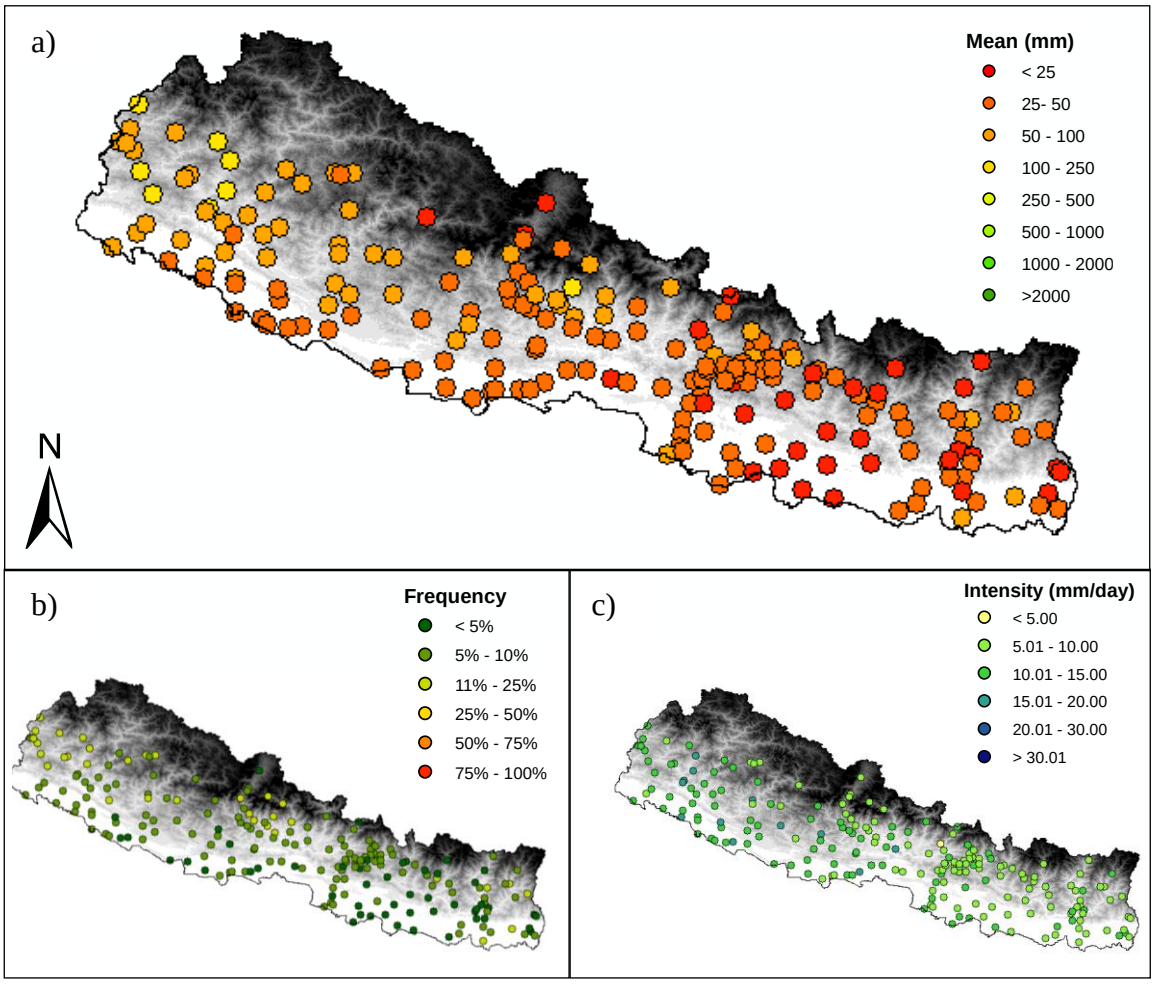

Figure 8. Winter season a) mean precipitation (mm), b) precipitation frequency (days), and c) precipitation event intensity (mm dy^{-1}) across the climatological period (1982-2011)

The winter season consists of 89 days that straddle the calendar year (65 days of the current year and 24 days at the end of the previous year). Mean precipitation across Nepal during the winter season is relatively light, with the majority of the gauges receiving between 25 and 50 mm. The greatest mean precipitation values are greater than 100 mm and are concentrated in the northwest regions of Nepal in the middle mountains. This supports the finding first made by Ichiyanagi et al. (2007) that western Nepal is characterized by greater precipitation than either the central or eastern regions during this season. The least amount of precipitation, less than 25 mm, occurs across the eastern third of Nepal, just east of Kathmandu. Regions of Nepal to the south and east are characterized by a relatively low frequency of precipitation than the remainder of the country during the winter season (Figure 8b), with less than 5% of the winter season characterized by days with precipitation. This is in contrast to the northwestern areas of Nepal, which are characterized by 10% - 25% of the days experiencing measurable precipitation. Due to the winter monsoonal influence, large weather systems tend to pass across the western portions of Nepal, which could explain the increased precipitation frequency and amount across northwestern Nepal during this season. Higher precipitation event intensities, ranging between 10 and 20 mm day^{-1}, are evident across the middle mountains and lowlands, mainly across the western half of Nepal. Lower intensities are found in the higher elevations and eastern Nepal. Lower intensity and less frequent precipitation events across the southeast could be influenced by the strong northeasterly flow that typically occurs during the winter monsoon. The winter season is characterized by the most stations with statistically significant precipitation trends, and all 14 of the stations with a significant trend were characterized by a decrease in precipitation ranging from 3.1 to 4.5 mm $year^{-1}$. The spatial distribution of these stations is across various elevations, with no identifiable spatial pattern to their location as they were distributed randomly across the country. Further, relative to the other seasons, precipitation in winter is not critical to the general annual hydroclimatology of Nepal given the low totals across the country.

3.4.3 Pre-Monsoon Season Analysis

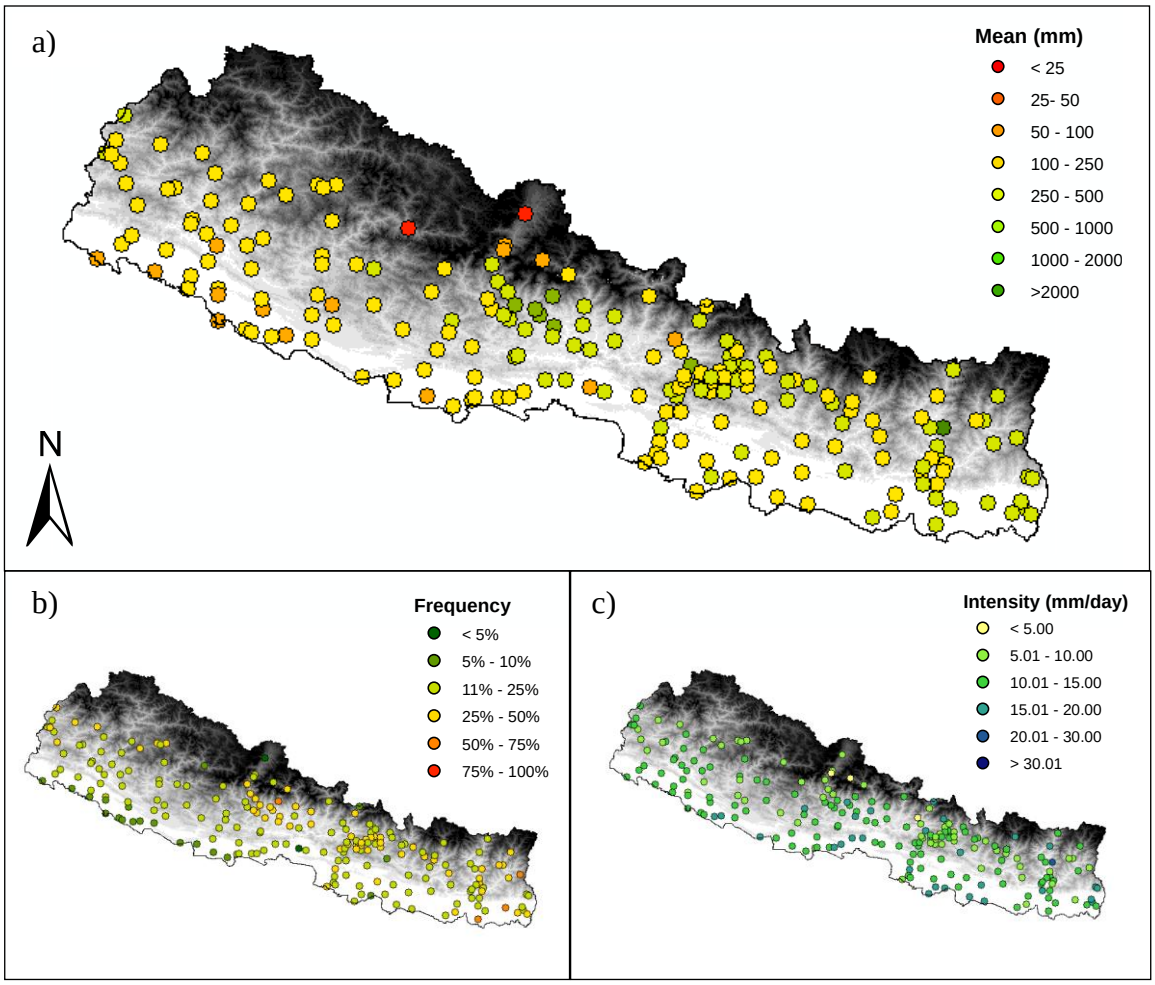

Figure 9. Pre-Monsoon season a) mean precipitation (mm), b) precipitation frequency (days), and c) precipitation event intensity (mm dy^{-1}) across the climatological period (1982-2011)

The pre-monsoon season is marked by generally more precipitation than the winter season across the country of Nepal (Figure 9a). The majority of the gauges measure between 100 and 300 mm of precipitation for the season. The precipitation differences during this season reveal a better-defined north-south precipitation gradient than during the winter season. The greatest mean precipitation, greater than 500 mm, is evident across the central portions of Nepal and extending to the east, supporting the results of Ichiyanagi et al. (2007). The least amount of precipitation occurs across the western lowlands and the central high mountains. The frequency of precipitation follows

a similar pattern to mean precipitation, with the smallest frequency (< 10 %) across the western lowland border regions and increasing with elevation to the high frequencies (25–50%) across the middle to high mountains (Figure 9b). The greatest frequency of precipitation events (50-75% of the days of the season) is concentrated in the far southeastern corner of Nepal, which could be attributed to the onset of the monsoon season, as it occurs first across this area. The intensity of precipitation events during the pre-monsoon season is significantly lower across the high mountain regions, where three gauges on average have observed less than 5 mm for each precipitation day historically. The precipitation gauges reflecting the greatest intensity of precipitation events, two standard deviations greater than the mean intensity calculated from all stations, are located from the lowlands to the middle and high mountain regions across southern and eastern Nepal. The influence of the impending summer monsoon is revealed through increased precipitation intensity and frequency across the southern and eastern regions of the country. Simple linear regression analysis revealed 9 stations with statistically significant precipitation trends across the 30-year period. The slope of the linear regression equation for each station revealed trends ranging from a decrease of 9.8 mm $year^{-1}$ to an increase of 14.1 mm $year^{-1}$. The spatial distribution of the stations seems to indicate a decrease in precipitation across the northwestern middle mountains, with increasing precipitation across the central interior and far eastern regions of Nepal.

3.4.4 Monsoon Season Analysis

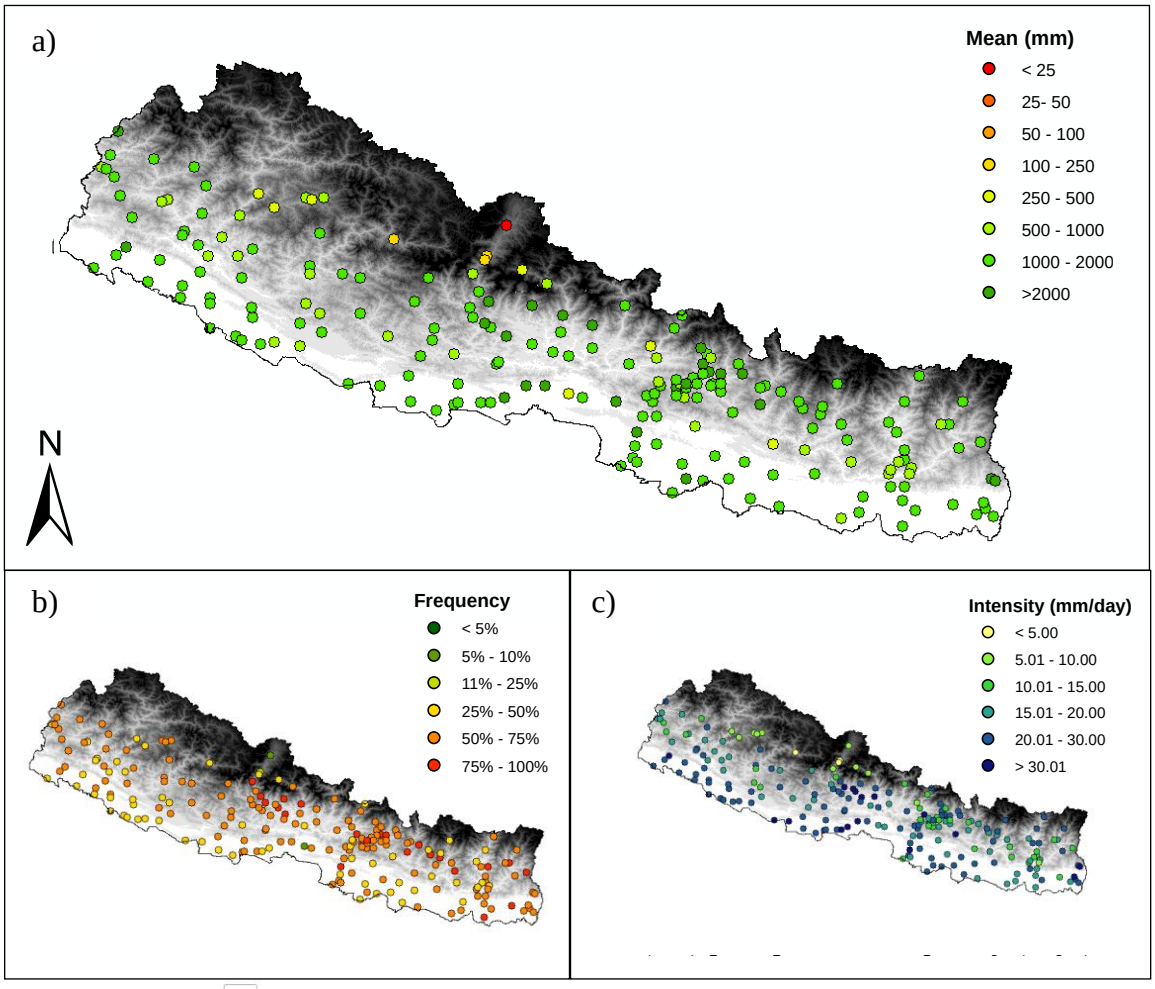

Figure 10. Monsoon season a) mean precipitation (mm), b) precipitation frequency (days), and c) precipitation event intensity (mm dy^{-1}) across the climatological period (1982-2011)

The monsoon season, defined here as extending across 122 days per year, is the season when Nepal, as a whole, receives close to 80% of its annual precipitation. The majority of the precipitation gauges (77%) record greater than 1000 mm for the season, on average. The smallest mean precipitation occurs in the central high-mountain/high-Himalaya regions, with an average of less than 250 mm. During this season, a strong flow of moist air continuously influences Nepal, translating to monsoonal rains, often in the form of strong thunderstorms. According to Wang (2006), precipitation amounts generally decrease from southeast to northwest, due to the moist air wedge gradually becoming thinner and dryer after the peak of the summer monsoon. This is supported by

the mean precipitation values across Nepal (Figure 10a), as the majority of the gauges across the southeastern half of Nepal are characterized by greater mean precipitation than the far northwest stations.

The frequency of precipitation (days) during the monsoon season is quite high, with the average gauge location experiencing precipitation on 58% of the days during the season, compared to 21% (pre-monsoon), 9% (post-monsoon), and 7% (winter) for the other three seasons. The smallest frequency of precipitation occurs throughout the lowlands along the southwestern border, with the greatest frequency (>75%) observed along the middle mountain regions of central and eastern Nepal. Even though there are fewer precipitation days across the lowland areas, the precipitation intensity across these areas is quite high, with one-half of the gauges characterized by the greatest daily intensity (> 30 mm day^{-1}; n=16) located in the lowlands, with the other half focused in the middle mountain region of Nepal. Precipitation intensity during the monsoon season seems to decrease with increased elevation (Figure 10c), as the intensity data closely follow changes in elevation. The stations with the greatest mean precipitation, frequency, and intensity are located across southeastern Nepal, which is where the bulk of the monsoon moisture tends to reside as this region is closest to the moisture source of the Bay of Bengal. Statistically significant precipitation trends during the monsoon season, as indicated by regression analysis, show great variation across the country. The trends range from a decrease of 23.9 mm $year^{-1}$ to an increase of 19.2 mm $year^{-1}$ with no noteworthy spatial patterns or clustering of stations across the country.

3.4.5 Post-Monsoon Season Analysis

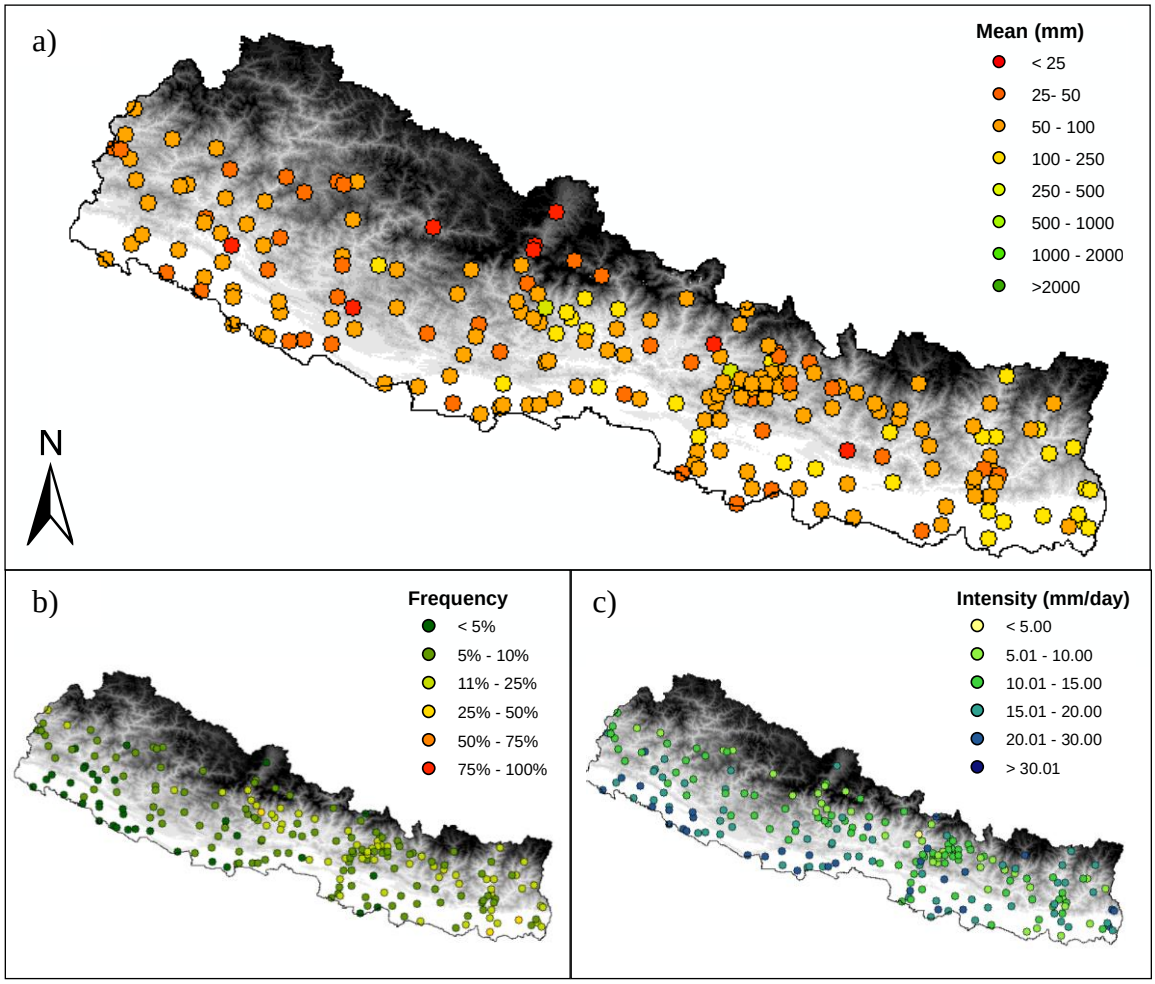

Figure 11. Post-Monsoon season a) mean precipitation (mm), b) precipitation frequency (days), and c) precipitation event intensity (mm dy^{-1}) across the climatological period (1982-2011)

Lastly, the post-monsoon season, which is the shortest season (61 days per year on average), is characterized by a retreat of the summer monsoon moisture. The disappearance of the moist monsoonal flow from the majority of the country is completed by late-October (Kansakar et al. 2004). The mean precipitation map (Figure 11a) reveals that the greatest precipitation occurs from the central through the far eastern portions of Nepal, with the two stations characterized by the greatest precipitation values located close to urban areas. The urban area surrounding Kathmandu experiences quite a

diversity in mean precipitation values during this season, with some stations less than 20 km apart characterized by mean precipitation of up to 50 mm difference, illustrating how varied precipitation can be across Nepal. The stations with the least amount of precipitation during this season (< 25mm) are located in the central high mountains and across the lowlands of the country. The smallest frequency of precipitation (Figure 11b) is confined to the lowlands in the northwestern regions, while the greatest precipitation frequency is located in the far southeastern lowlands. This arrangement of precipitation frequency corresponds with the pattern of precipitation during this time period, as the monsoon moisture still tends to influence the southeastern regions. The majority of the gauges are characterized by precipitation during 4-9% of the days of the season, with the most frequent being 30%. The precipitation stations characterized by the greatest frequency (Figure 11b), are among those with the lowest precipitation event intensity (Figure 11c). This finding indicates that for those particular locations, precipitation during the post-monsoon season is light and frequent. The greatest precipitation intensity tends to be across the lowlands and into the middle mountain regions of central and western Nepal. Only three stations exhibited statistically significant precipitation trends during the post-monsoon season and all are located in the eastern half of Nepal. These trends ranged from a slight decrease of 2.7 mm $year^{-1}$ to an increase of 5.3 mm $year^{-1}$.

3.4.6 Temporal Analysis of Seasonal Precipitation

Seasonal observations from all of the precipitation gauges across Nepal were analyzed to illustrate the general country-wide temporal variation of seasonal precipitation. The standard deviation for each of the seasons was assessed and the values reveal that the monsoon season is characterized by the greatest seasonal variation over the climatological period (257.2mm), followed by the post-monsoon (145.7mm), pre-monsoon (109.2mm), and winter (72.0mm) seasons. As standard deviation is a function of the magnitude of the variable, it is not surprising that the greatest standard deviation is for the very wet monsoon season. To normalize this variability the coefficient of variation could be applied by dividing the standard deivation by the mean. Since these seasonal precipiation observations take into account the entire country of Nepal, the varying duration of the influence of the summer monsoon may influence the high variablilty during that season.

Seasonal precipitation frequency and intensity are evaluated to uncover any patterns in the precipitation occurrences over Nepal. The greatest variance in precipitation frequency (%) is evident in the pre-monsoon and monsoon seasons, both with a standard deviation of 0.04%, followed by the post-monsoon (0.03%) and winter (0.02%) seasons. These deviations indicate that the mean Nepal-wide frequency of precipitation for each season is not highly variable from year-to-year. The general trend in the frequency of precipitation is negative for all seasons, with the monsoon season showing the greatest change in frequency with a statistically significant slope of -0.01 %/year. The coefficient of determination of the monsoon frequency over time shows that time (year) explains 12% of the variance in precipitation frequency. The evaluation of intensity across Nepal shows no significant trends over time for any of the precipitation-defined seasons. The post-monsoon season showed the greatest annual intensity variance, which could be attributed to the variability in the timing of the retreat of the monsoon moisture from Nepal during this season. It is concluded that no strong trend in precipitation frequency occurred during the study period across Nepal.

3.4.7 Elevation Analysis

The elevation distribution of the precipitation gauges across Nepal is important to note prior to analyzing any precipitation patterns for a relationship with elevation. There is diversity in elevation for the 210 precipitation gauges used in this study (Figure 12a). The majority of the stations used to construct the climatology are below 2000 meters, with over 70 gauges located at less than 500 meters and only three gauges positioned at greater than 3000 meters elevation.

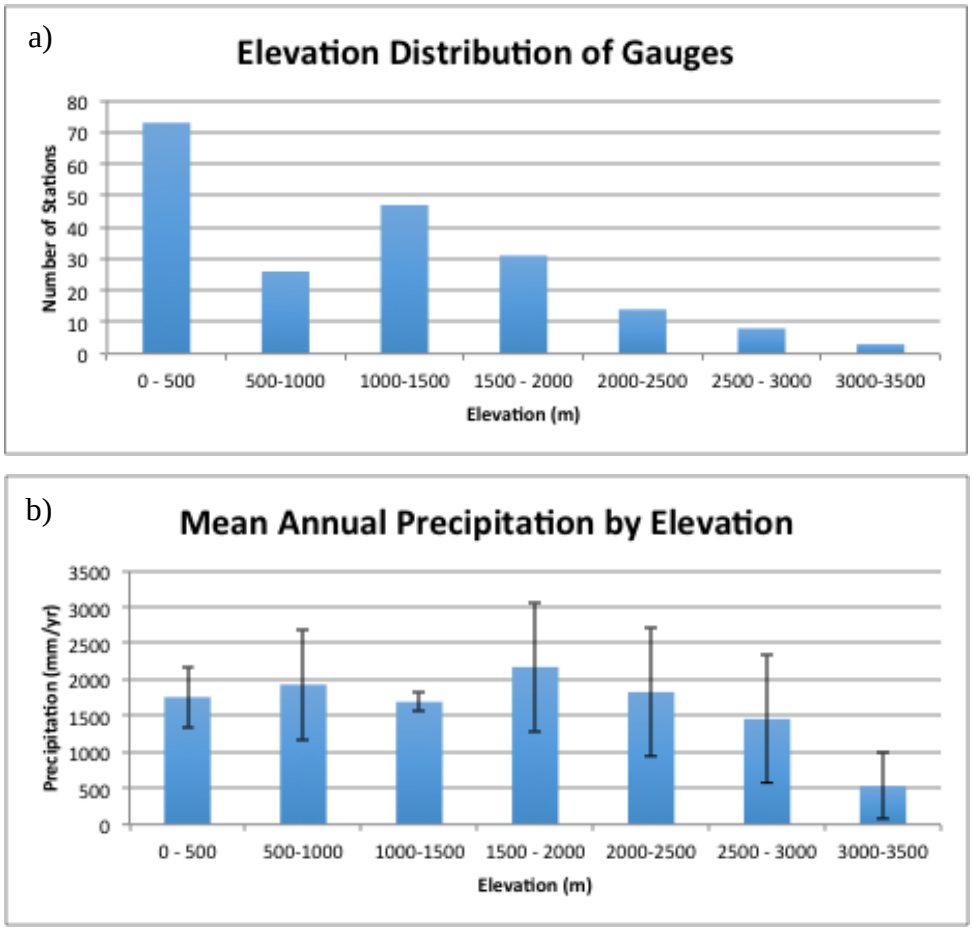

Figure 12. a) Number of precipitation gauges in each 500-meter elevation bin and b) mean annual precipitation (bars) across all stations for each elevation bin with 2 times the standard deviation indicated above and below the means (vertical lines).

The greatest mean annual precipitation is found between 1500 and 2000 meters, with the least amount of annual precipitation occurring at the higher elevation bin, above 3000 meters (Figure 12b). This may be related to the concept that elevation enhances precipitation to a degree, but above a certain elevation the low air temperatures and lack of available moisture may inhibit precipitation. However, the station density (Figure 12a) may also contribute to the lesser precipitation and higher standard deviation at higher elevations. The smallest standard deviation for mean annual precipitation occurs in the 1000 – 1500 meter bin, showing significantly less variance at these elevations. Keeping in mind a coefficient of variation analysis may yeild a more telling result since that would be a normalizaion of the mean annual precipitation A linear regression analysis was performed using the mean precipitation data for each station and for each season and station elevation in order to identify any signifcant relationships between mean station

precipitation and elevation. The only season that indicated a statistically significant trend (p-value ≤ 0.05) when using normalized seasonal preciptiation means was the monsoon season. The slope of the regression equation indicates a decrease of precipitation with increasing elevation (-1.9 mm m^{-1}) .

3.5 Conclusion

The climatological patterns and trends in precipitation across Nepal are summarized in order to build a foundation for the verification analysis. As expected the monsoon season is characterized by the greatest mean precipitation, precipitation intensity, and frequency. The least amount of precipitation is observed during the winter season, with the majority of the precipitation during that season located across the northwest regions. During the pre-monsoon and post-monsoon seasons, the greatest precipitation frequency and intensity tend to occur across the southeastern portions of Nepal, as the monsoonal flow enters first and departs last over this region of Nepal. Overall the majority of the precipitation patterns seem to be influenced greatly by the spatial distribution of the moist monsoon air across Nepal. There is some influence on precipitation by elevation across Nepal, but the lack of gauge density at the highest elevations needs to be considered. The most significant relationship between elevation and precipitation amount occurs during the monsoon season. After analyzing the climatological trends and precipitation means, a foundation has been laid for the verification of the TRMM satellite across Nepal.

CHAPTER 4

TRMM Verification

4.1 Data

4.1.1 TRMM Satellite Data

The TRMM satellite data used for this study are the TRMM 3B42 daily accumulated rainfall estimates, which were made using version 7 algorithms. The TRMM version 7 algorithms blend-in additional satellite data while utilizing improved resolution and aerial coverage of the infrared data used in the previous version of the algorithm (Chen et al. 2013). The TRMM 3B42 data have a 24-hour temporal resolution with the data representing precipitation accumulation during the period 2230 UTC of the previous day to 2229 UTC of the current day, which translates to 4:15am to 4:14am Nepalese standard time. TRMM reports at a spatial resolution of 0.25 degrees latitude by 0.25 degrees longitude. The 3B42 V7 daily accumulated TRMM data are derived from the 3-hourly 3B42 V7 precipitation estimates. Of the 266 TRMM grid cells that cover Nepal, only 141 are co-located with precipitation gauges, and as such only these cells were used in this analysis (Figure 13). The raw TRMM 3B42 data were not processed in any way, as the objective of this study is a basic evaluation of raw TRMM precipitation estimates across Nepal. These satellite-derived daily precipitation data are freely available through NASA's TRMM Online Visualization and Analysis System, or TOVAS (http://gdata1.sci.gsfc.nasa.gov/daac-bin/G3/gui.cgi?instance_id=TRMM_3B42_Daily). Data for all 141 grid cells are greater than 90% complete for the study period, showing a reasonably complete and reliable dataset for the 1998 – 2011 period.

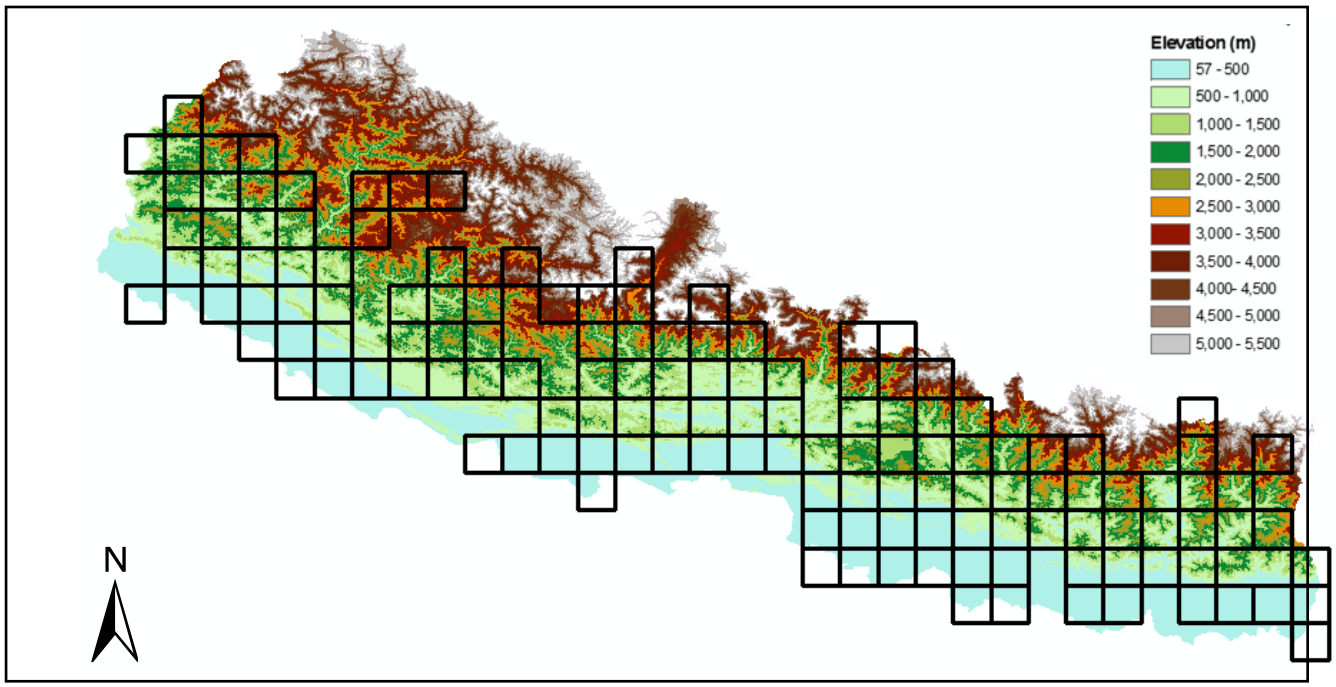

Figure 13. TRMM grid cells used in the verification process overlayed onto Nepal elevation data.

4.1.2 Precipitation Gauge Data

A relatively dense network of weather stations across Nepal that is maintained by the Nepalese government was used to verify TRMM satellite-derived precipitation estimates. The rain gauge measurements are provided by the government of Nepal from the Department of Hydrology and Meteorology in the Ministry of Science, Technology and Environment. Access to the weather station precipitation data weas graciously provided by Dr. Netra Chhetri of Arizona State University. This dataset includes daily rain gauge measurements for 286 weather stations, along with the exact elevation and approximate location for each station. Few of the stations across Nepal have a data record that extends as far back as the year 1947. The Nepalese rain gauge network represents a wide array of elevations, with 32% of the stations located below 500m and 15% located above 2000m. The spatial distribution of these stations reveals that they are concentrated among more populated areas, such as the capital city Kathmandu, and regions of lower elevation. This study only incorporates data for weather stations which have 90% or more data completeness for the period of study in order to ensure a robust analysis.

The possible errors with precipitation gauge measurements previously summarized by Wang and Wolff (2010) and Nespor and Sevruk (1999), may cause inaccurate measurement of precipitation data, and this presents a caveat when relying on point rain gauge data for this validation. It is possible to perform spatial interpolation of the rain gauge data by using methods such as distance decay while accounting for elevation differences, but the interpolated data will nonetheless be a coarse estimate. Interpolation in an area of complex terrain, such as Nepal, raises concerns over data inaccuracies given the typical inhomogeneity of precipitation in general, but particularly in areas of complex topography. Some studies such as that by Duncan and Biggs (2012) use interpolated rain gauge data to produce a gridded precipitation product; however, this approach may skew the data since point rain gauge data are only valid for a specific station location. Therefore, the gauge data were left as point representations of precipitation rather than attempting to interpolate the data to match the TRMM grids.

The precise temporal resolution of the precipitation gauge data and the instrumentation used for measurement are rather uncertain, as little metadata are provided with the dataset. The station data were described as collected on a daily basis, but no consistent observation time was provided. Because of this uncertainty in the data, and the lack of knowledge of how the rain gauge measurements were recorded, one "day" of gauge precipitation will be assumed to include the precipitation from 12:00 am to 11:59 pm Nepalese standard time (NST). The type of precipitation gauge used across Nepal is also unknown, but it will be assumed that the gauges are manual and not automated. Since the gauges are assumed to be manual, it is suspected that observer times varied, and this led to the investigation of multi-day averages in order to account for the likelihood of different observation times and to account for the odd 24-hour period that daily TRMM data represent.

The raw gauge data were evaluated in order to address any data issues before any verification analyses were completed. First, data flags included in the data set were considered: if the rain gauge was not working properly a "Data Not Available" (DNA) reading was recorded; if the station was not yet installed or had been uninstalled, a blank

value was given for that individual station for that particular time. When analyzing for data completeness, a station must have reported valid (i.e., non-missing) precipitation measurements for 90% or greater of the days during the 14-year study period in order to be included in the analyses. For the years 1998-2011, coinciding with the TRMM data record, 220 of 286 stations (77%) were deemed to have 90% or greater data completeness. The station data were quality controlled by flagging all observations that appeared as statistical outliers, which was defined here as a daily precipitation total greater than 2.5 standard deviations above the mean. Such anomalous daily precipitation values were validated against observations from nearby stations. The majority of the daily data fell within the threshold of 2.5 standard deviations, though several days were investigated to further validate the gauge observations. Since the gauges are somewhat spread spatially, and the elevation across Nepal changes drastically across short distances, only gauges within 20 km of each other were used to validate the daily observations. Few days were eliminated, but this elimination of data still kept all 220 stations at greater than or equal to 90% data completeness.

4.1.3 Elevation Data

Elevation plays an important role in precipitation formation and inhibition, and therefore elevation data were needed to assess the validity of TRMM as related to elevation. Two sources were used as elevation data in this verification analysis. Digital elevation data from the Shuttle Radar Topographic Mission (SRTM), originally produced by NASA, were used as the primary elevation dataset. The SRTM data have a resolution of 90 meters at the equator and they were imported into ArcGIS for statistical analysis. Zonal statistics were performed on the SRTM DEM to find the mean elevation across each grid cell within Nepal. The other elevation data used in the verification of TRMM was the precipitation gauge elevation, which was provided by the Nepalese Department of Hydrology and Meteorology. The gauge elevation data were used to evaluate any statistically significant trends in the TRMM accuracy as related to elevation.

4.2 Methods

4.2.1 Spatial Uncertainty

Nepalese weather station precipitation amounts through the 14-year period were compared to TRMM precipitation estimates on a point-by-pixel basis. Because of the extreme differences in the spatial distribution of convective precipitation that is typical of the warm, moist season within a monsoon regime, it is important to use the rain gauge data as a point data source, and not as an indicator of exact surrounding precipitation amounts (Wang and Wolff 2010). Compounding the issue here is that the locational information for stations within the Nepalese network is not highly precise – latitude and longitude values are provided in degrees and whole minutes only. This uncertainty issue is likely due to differences in the type of coordinate systems used in Nepal as translated to the decimal degree and degrees, minutes, seconds, systems used in the United States and elsewhere. This location issue is deemed acceptable for this study since the stations are being referenced to a rather course satellite-data grid (0.25°). In order to mitigate this positioning problem, a 60 arc-second buffer was applied to each weather station point using ArcGIS. The addition of a buffer outlined the possible region where the actual Nepalese weather station may be located. These station points, along with their corresponding buffer regions, were overlain onto the TRMM data grid in ArcMap in order to precisely align the locations of these datasets. If any portion of a weather station buffer was located within the bounds of a TRMM data cell it was included in the verification process for that TRMM pixel. Therefore, a single precipitation gauge could be compared to more than one TRMM cell. The verification was conducted through direct comparison of the TRMM satellite precipitation estimate to the simple mean precipitation of all stations within each grid cell, with no weighting scheme applied. Only the TRMM cells (n=141) that contain at least one weather station were included in the analysis.

4.2.2 Temporal Inconsistencies

The temporal resolution of the TRMM data as calculated in Nepalese standard time covers a 24-hour time period beginning at 4:15 am on the current day. As stated

previously, it is assumed that the rain gauge precipitation data encompass a 24-hour time period beginning at 12 am and ending at 11:59 pm NST of the current day. This reveals problems when trying to make a direct comparison between TRMM estimates to the rain gauge data. When referencing TRMM data to individual calendar days, one day of accumulated precipitation in Nepal would be missing the four hours and fifteen minutes after midnight of the current day, while also accumulating four hours and fifteen minutes of the following day. This day-to-day overlap needed to be addressed before verification of the TRMM data using daily precipitation gauge data could be conducted.

The problems resulting from the temporal misalignment, along with the inconsistencies in rain gauge data observation times prompted an investigation of multi-day running means. Various running means (3-day, 5-day, 7-day, 9-day, 11-day, and 13-day) were calculated for the TRMM estimations and rain gauge measurements for the entire time period. Basic statistical analyses were performed on these running averages in order to find the best timeframe for TRMM-gauge comparison. The statistical analyses included correlation coefficient, index of agreement (D-statistic), and mean absolute error, which are graphically represented by season in Figure 14 (a-c). The correlation coefficient measures the co-variability of the TRMM estimation and the rain gauge observations for the various running means. The index of agreement, developed by Willmott (1981), is a standard measure of the degree of prediction error (Moriasi et al. 2007). The mean absolute error is based on the absolute value of TRMM-gauge differences, which is preferred to those statistical measures of error based on squared differences (Willmott et al. 2011).

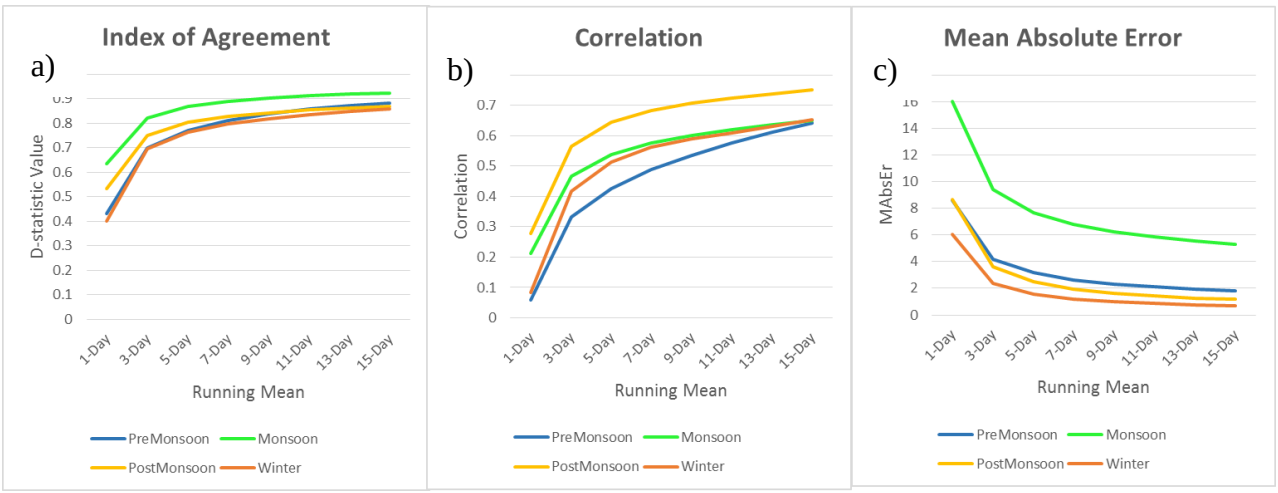

Figure 14. Statistical analyses comparing TRMM with gauge observations completed for each running mean threshold. Statistics included are a) D-statistic or index of agreement, b) correlation, and c) mean absolute error.

The three statistical analyses were evaluated in order to identify the running mean that appears to best account for the temporal inconsistencies between TRMM and precipitation gauge data. As expected the correlation coefficient and the index of agreement between TRMM and the station precipitation increase as more days are included in the running average. After visual interpretation of the statistics generated for the running means, the largest inflection point on all three of the graphs depicting the statistical measures occurs at the 3-day running mean. This analysis indicates that the running means produced beyond three days only offer a slight improvement to the agreement and correlation of the data. As the TRMM 24-hour time period does not aligning exactly with the daily rain gauge data, the one day analysis is not expected to offer coincidental measures of precipitation. Conversely, since the TRMM – rain gauge observations should be misaligned by less than two days, the 3-day running mean offers the most sensible solution and the statistics seem to support this conclusion. Therefore, only the 3-day running mean was used in the verification of TRMM satellite estimates across Nepal.

4.2.3 Statistical Analyses

The TRMM estimations are assessed against gauge data on monthly, seasonal, and annual time scales in order to achieve a broad assessment of TRMM accuracy using

the 3-day running means across Nepal. The analysis of the TRMM data at its original resolution focuses on the quality of the 3B42 daily accumulated precipitation as compared to the Nepalese rain gauge network. To characterize the spatial and temporal relationships between TRMM estimates and gauge data, an array of model evaluation statistics were generated for each season, including mean error, mean absolute error, root mean squared error, correlation coefficient, and index of agreement.

The root mean squared error (RMSE) and mean absolute error (MAE) are calculated as

$$RMSE = \sqrt{\frac{\sum_{i=1}^{N}(T_i - G_i)^2}{N}}$$

and

$$MAE = \frac{\sum_{i=1}^{N}|T_i - G_i|}{N}.$$

In these equations T and G are TRMM estimates and rain gauge measurements respectively, where N is the number of daily observations.

Systematic and unsystematic RMSE values (RMSEs and RMSEu) are also calculated in order to establish the degree of bias or systematic error (RMSEs) versus random or unsystematic error (RMSEu) when using TRMM data as a predictor of gauge data (Willmott and Matsuura, 2005). These RMSE evaluations are calculated as,

$$RMSEs = \sqrt{\frac{\sum_{i=1}^{N}(\hat{T}_i - G_i)^2}{N}}$$

$$RMSEu = \sqrt{\frac{\sum_{i=1}^{N}(T_i - T)^2}{N}}$$

using $T_i = a + bG_i$, where the *a* and *b* parameters related to an ordinary least squares simple linear regression between the TRMM estimate and the rain gauge measurements (Willmott, 1984).

The standard deviation of the TRMM satellite estimate (S_t) is calculated as

$$S_t = \sqrt{\frac{\sum_{i=1}^{N}(T_i - \bar{T})^2}{N}}.$$

In this equation T_i is the TRMM precipitation estimate, and the mean of the TRMM precipitation value is $\bar{T}$. Similarly the standard deviation of the gauge data (S_g) is calculated with G_i as the rain gauge measurement, and $\bar{G}$ being the mean gauge measurement in the equation

$$S_g = \sqrt{\frac{\sum_{i=1}^{N}(G_i - \bar{G})^2}{N}}.$$

The correlation coefficient (r) is calculated to reflect the co-variability of the TRMM satellite and the rain gauge data (Hanson et al. 1992). The correlation coefficient varies from -1, a perfect inverse relationship, to +1, a perfect direct relationship, and is calculated as

$$r = \frac{\frac{\sum_{i=1}^{N} T_i G_i}{N} - \bar{T}\bar{G}}{S_p S_o}.$$

Another statistical measure of verification is the index of agreement (D or IOA). The range of this statistic is from 0 to 1, with 1 indicating a perfect agreement between the TRMM satellite estimate and the rain gauge measurement. Unlike the correlation coefficient, the index of agreement accounts for the magnitude of the difference between the TRMM satellite precipitation estimate and the rain gauge recorded precipitation, whereas the correlation coefficient only represents the co-variability of the two types of data. The index of agreement is calculated as

$$D = 1 - (N)\frac{RMSE^2}{PE}.$$

In this calculation PE is defined as

$$PE = \sum_{i=1}^{N} (|T_i'| - |G_i'|)^2$$

and

$$T_i' = T_i - \bar{G} \qquad G_i' = G_i - \bar{G}.$$

Three additional parameters were evaluated for each TRMM grid cell across all four seasons of Nepal's climate. Table 2, adapted from Scheel et al. (2011), describes the variables used to formulate the frequency bias index, false alarm ratio, and the probability of detection of the TRMM satellite precipitation estimates.

	Gauges rain	Gauges no-rain
TRMM rain	a	b
TRMM no-rain	c	d

Table 2. Variables used to quantify the relationship between the precipitation gauges and the TRMM data based on precipitation occurrence adapted from Scheel et al. (2011).

The frequency bias index (FBI) gives the ratio of TRMM satellite rain estimates to the actual precipitation events as reported by the weather stations across Nepal. For this index a value less than 1 indicates an underestimation of precipitation frequency by TRMM, while any value greater than 1 indicates an overestimation of precipitation frequency by the TRMM satellite estimations. The FBI is calculated as

$$FBI = \frac{(a+b)}{(a+c)}.$$

The false alarm ratio (FAR) measures the fraction of false precipitation occurrences indicated by the TRMM product estimations. The FAR assesses the number of instances where the TRMM satellite indicated that precipitation occurred within a grid cell when zero precipitation was reported at all of the weather stations within that cell. The FAR is defined as

$$FAR = \frac{b}{(a+b)}$$

using the parameters *a* and *b* from Table 2.

The probability of detection (POD) computes the fraction of daily rain events that were properly identified by the satellite. Referring to the variables *a* and *c* from Table 2, the POD is calculated using as

$$POD = \frac{a}{(a+c)}.$$

These three additional parameters were then imported into ArcGIS to provide a better understanding of the spatial distribution of the statistical values across the TRMM grid cells.

4.2.4 Kathmandu Case Study

The majority of the TRMM grid cells used in this verification, specifically 82%, each contains less than 3 precipitation gauges. Since each grid cell covers an area of approximately 575 kilometers, it would be more beneficial to have a higher number of weather stations within each cell. An increased number of stations within a grid cell decreases the difference between the mean observed rainfall within the grid cell and the TRMM satellite estimate (Hazarika et al. 2007); therefore, a case study of the grid cell containing the most precipitation gauges was performed. The grid cell that contains the capital city of Kathmandu includes 13 precipitation gauge buffer regions (Figure 15). Since this cell contains such a relatively high number of stations it is expected to offer the most reliable depiction of the of the TRMM-gauge relationship.

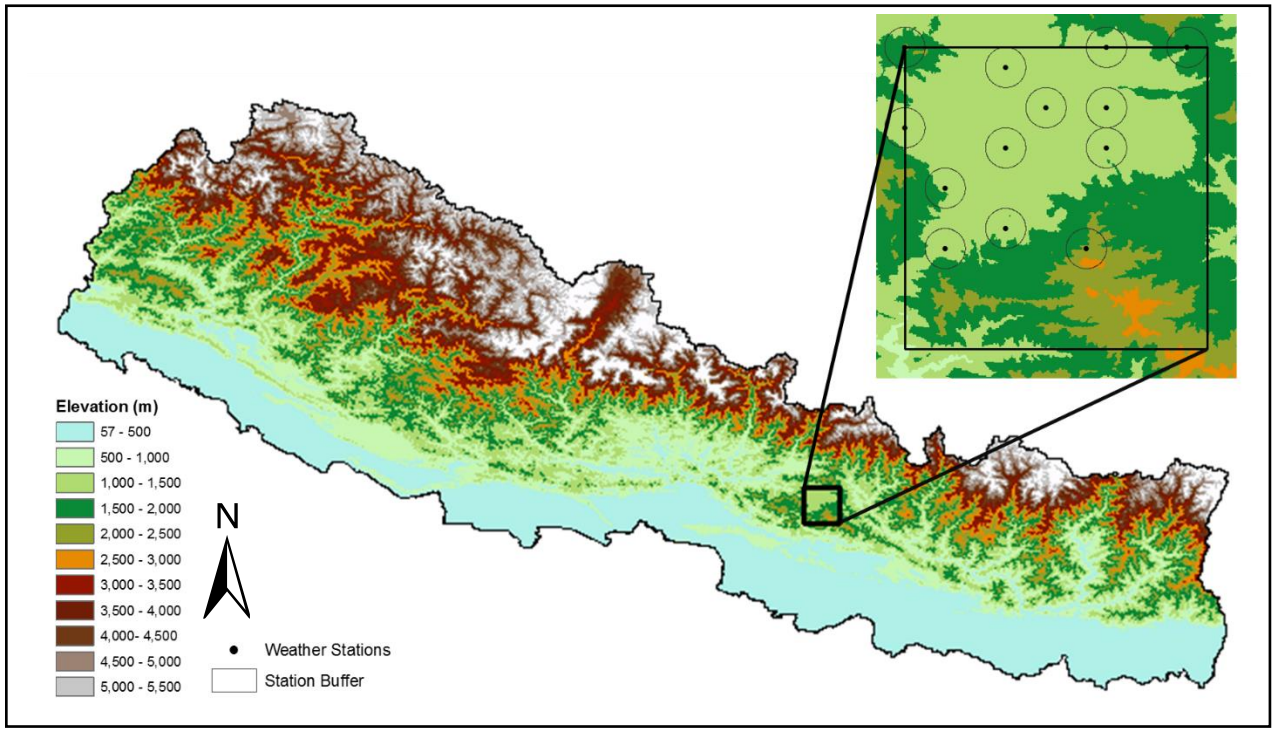

Figure 15. Elevation across Nepal and the location of the TRMM grid cell co-located with 13 precipitation gauges (inset) used for TRMM verification case study.

To assess the accuracy of TRMM data over the Kathamandu grid cell, a more detailed analysis was performed. This analysis included the comparison of the TRMM precipitation estimates to the station observations using the 3-day running mean on a seasonal and yearly time scale.

Extreme precipitation events are a great cause for concern for Nepalese citizens, as these types of events are the main cause of natural disasters in Nepal. Therefore, it is important for any type of precipitation estimation tools to be able to accurately estimate high precipitation events. The assessment of the TRMM data accuracy for extreme precipitation events was validated by examining the 10 greatest daily precipitation amounts as indicated by the TRMM satellite and the 10 greatest precipitation observations as indicated by the gauges for each of the four seasons. For each of the

greatest precipitation days, the mean, maximum, minimum, and standard deviation of the 13 gauge precipitation observations were compared to the TRMM estimate.

Additionally, the bias of TRMM data as a function of rain-gauge amounts was also calculated for the case study grid cell. This bias evaluation was performed previously by Scheel et al. (2011) in their TRMM validation study for the Central Andes in South America. A bias assessment based on station observations is used in order to indicate any bias across varying daily precipitation totals (< 0.1mm, 0.1-0.2mm, 0.2-0.5mm, 0.5-1mm, 1-2mm, 2-5mm, 5-10mm, 10-20mm, and >20mm). The bias calculation evaluates the average difference between the TRMM satellite estimate and the corresponding precipitation gauge value and is calculated as follows:

$$BIAS = \frac{1}{n}\sum_{i=1}^{n}(Z^{TRMM}(x_i) - Z^{gauge}(x_i))$$

Where Z^{TRMM} is the TRMM daily precipitation accumulation amount, Z^{gauge} is the corresponding average gauge precipitation within that grid cell, and n is the number of days (Scheel et al. 2011). This metric is used to identify overestimations and underestimations within the various precipitation categories defined above in order to identify any systematic biases.

Finally, the daily mean and daily standard deviation were calculated from each precipitation gauge within the Kathmandu case study grid cell. In order to have good daily data, at least 11 of the 13 gauges (85%) had to report a precipitation observation on that day. The daily standard deviation of precipitation across the 13 gauges is calculated as

$$\sigma = \sqrt{\frac{1}{N}\sum_{i=1}^{N}(x_i - \mu)^2}$$

where μ is the simple mean of the daily precipitation as reported by the 13 (N) gauges. This formula will also be used for various other standard deviation calculations as indicated in the results section. Finally, the maximum, minimum, and mean daily standard deviations for each season are calculated in order to illustrate the typical variability in daily precipitation across the Kathmandu grid cell.

The methods outlined here yielded statistics and information that were depicted using graphs, charts, and maps to visualize any spatial or temporal patterns in accuracy of the TRMM satellite across Nepal. Many of the methods used in the verification of the TRMM satellite estimations have been used in other various TRMM verification studies for other parts of the world (Scheel et al. 2011; Duncan and Biggs, 2012; Chen et al. 2013). A case study is included in the verification analysis to give a more detailed account of the TRMM accountability across Nepal's most populated (in terms of people and rain gauges) region. The spatial and temporal uncertainties associated with the data were addressed first, followed by the verification analysis.

4.3 Results

Presented in this section are the results of the statistical analyses used to assess the ability of the TRMM system to estimate precipitation across Nepal using data from the period 1998 – 2011. The analyses here focused on the quality of the daily TRMM data product on a 0.25 x 0.25 degree resolution as compared to the precipitation gauge observations on a point-by-grid basis. The results are presented spatially and temporally, through various tables, graphs, and maps in order to depict and characterize the most important findings.

The most telling of the statistical analyses were examined and mapped via ArcMap 10.2 for each TRMM grid cell to show the spatial depiction of the statistics. Two things were kept in mind when analyzing the map statistics: average elevation across the grid cell and the number of gauges within each grid cell. The pattern of elevation across Nepal shows low elevations (< 500m) across the southern and western border regions, with increasing elevation progressing from southwest to northeast (Figure 16a). The density of the precipitation gauges across Nepal demonstrates the lack of multiple rain gauges for the majority of the grid cells (Figure 16b). Over one-half, specifically 60%, of the grid cells used in this analysis contain only one precipitation gauge, with only seven grid cells encompassing more than four gauges.

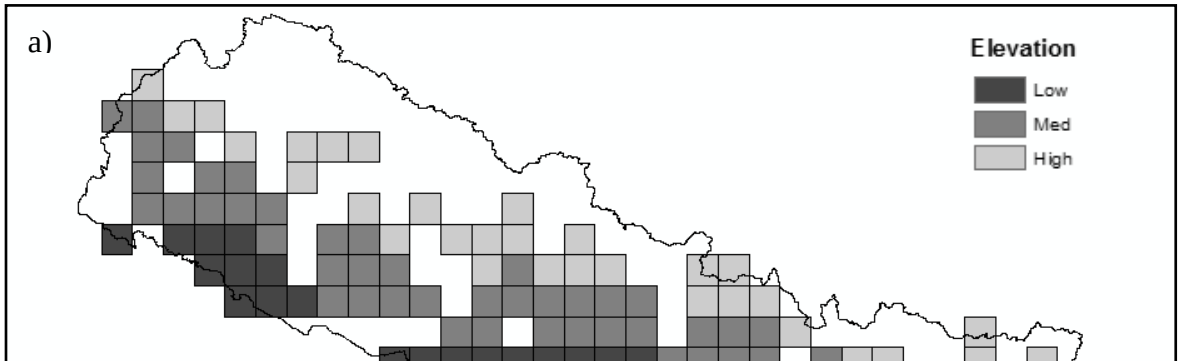

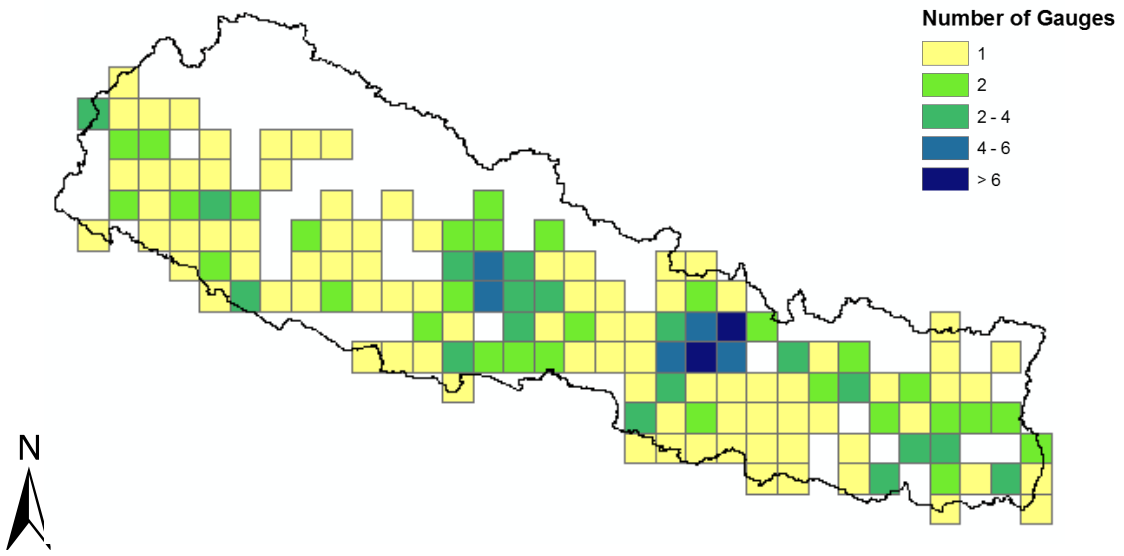

Figure 16. Elevation categories for the average elevation within each TRMM grid cell across Nepal: low <500m, medium 500m - 1500m, high > 1500m (a) and density of precipitation gauges for each TRMM grid cell (b).

4.3.1 Verification Statistics

The statistical results illustrate differences in the accuracy of TRMM data on a seasonal basis (Table 3; Figure 17). During the hydrologically important monsoon season, TRMM data underestimate precipitation across Nepal, which supports the findings by Scheel et al. (2011) that higher intensity precipitation events are generally underestimated during the wetter seasons. According to Scheel et al. (2011) RMSE values tend to be higher during the wet season, which is partly due to greater precipitation during this season, which is again supported by the results found here (Table 3). The higher frequency of precipitation events during the monsoon season helps to explain the low false alarm ratio and high probability of detection across Nepal. The winter and post-monsoon seasons are characterized by a fairly high false alarm ratio of 0.51 and 0.41

respectively, which is supported by high frequency bias indices for both of those seasons. Since the frequency bias index values for both the pre-monsoon and monsoon seasons are less than one, this indicates an overall underestimation by TRMM, while the winter and post-monsoon FBI values signify an overestimation. Seasonal correlation coefficients reveal that the association of TRMM estimates with the gauge data is greatest during the monsoon season. This shows that gauge-TRMM covariance for total precipitation amount is high during the monsoon season, possibly as a function of the increased precipitation events during that time of year. TRMM appears to be rather effective at estimating seasonal precipitation as verified by the gauge data, and will be investigated further through a spatial analysis of the aforementioned statistics.

	Pre-Monsoon	**Monsoon**	**Post Monsoon**	**Winter**
Sample Size	1204	1708	896	1305
Mean TRMM (mm/day)	4.1	12.4	3.3	1.9
Mean Gauges (mm/day)	3.9	12.6	3.4	2.1
TRMM Standard Deviation (mm/day)	5.2	13.0	4.6	2.5
Gauge Standard Deviation (mm/day)	3.9	8.4	3.8	2.9
RMSE (mm/day)	4.8	10.8	4.0	2.7
RMSEs (mm/day)	1.4	3.7	1.3	1.6
RMSEu (mm/day)	4.7	12.6	3.9	2.2
Mean Absolute Error (mm/day)	3.1	7.4	2.0	1.5
Correlation Coefficient	0.49	0.63	0.57	0.51
Index of Agreement (IOA)	0.80	0.88	0.78	0.76
False Alarm Ratio (FAR)	0.09	0.01	0.41	0.51
Frequency Bias Index (FBI)	0.92	0.99	1.03	1.02
Probability of Detection (POD)	0.84	0.98	0.61	0.50

Table 3. Statistical results for seasonal TRMM data, gauge data, and TRMM-gauge validation. RMSE refers to root mean squared error, for which systematic (RMSEs) and unsystematic (RMSEu) values are also reported.

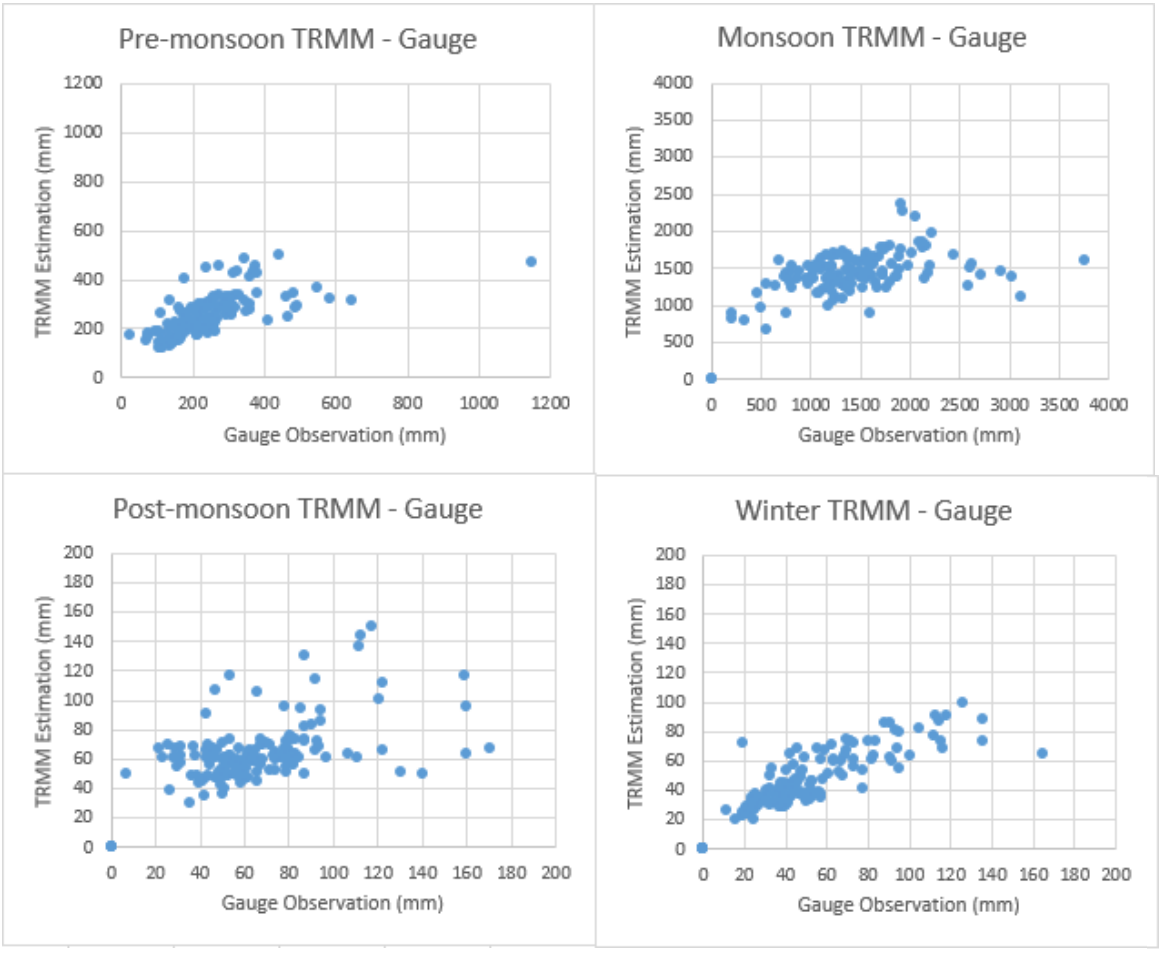

Figure 17. TRMM – gauge scatter plots for the pre-monsoon (a), monsoon (b), post-monsoon (c), and winter (d) seasons.

4.3.2 Pre-Monsoon Season

The pre-monsoon season is characterized by a spatial pattern to each statistic, with indications of an elevation influence. During the pre-monsoon season the index of agreement (IOA) is generally lower across the higher elevations to the north and across the central regions (Figure 18a). The majority of the TRMM grid cells indicate an overestimation by TRMM according to the FBI, with slight underestimations concentrated in the middle to high elevations of the eastern half of the country (Figure 18b). The POD is smaller during the pre-monsoon season period than during the

monsoon season. The low false alarm ratios towards the center of Nepal indicated in Figure 5d visually correspond to the density of precipitation gauges from Figure 16b. Low false alarm ratios are also concentrated across the far eastern portion of Nepal, which may correspond to the increased precipitation in that region due to the variation in the summer monsoon onset date. Statistically significant correlations between the values of the statistical results and elevation were found for the IOA and POD during the pre-monsoon season (Figure 19b; Figure 19d). Simple regression analysis indicates increasing POD with elevation, while regression analysis for the IOA showed a slight decrease in agreement with elevation (Figure 19b).

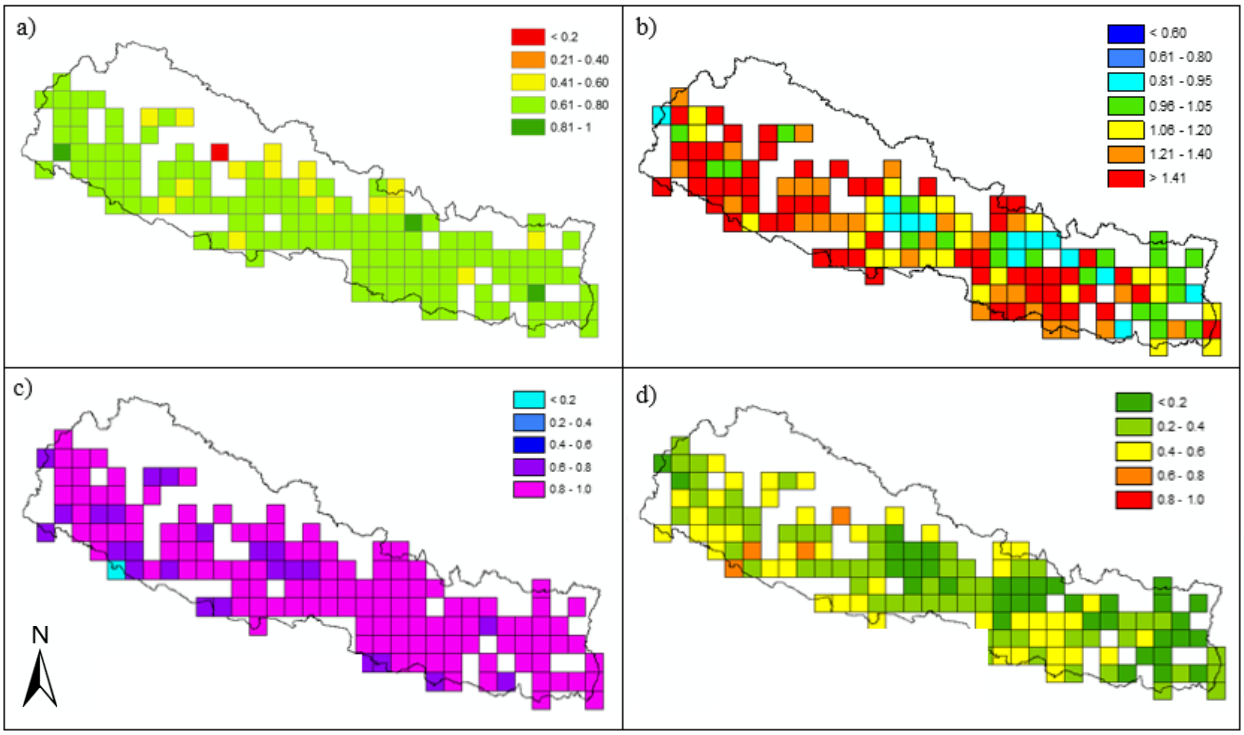

Figure 18. Pre-monsoon seasonal verification statistics, including a) index of agreement, b) frequency bias index, c) probability of detection, d) false alarm ratio.

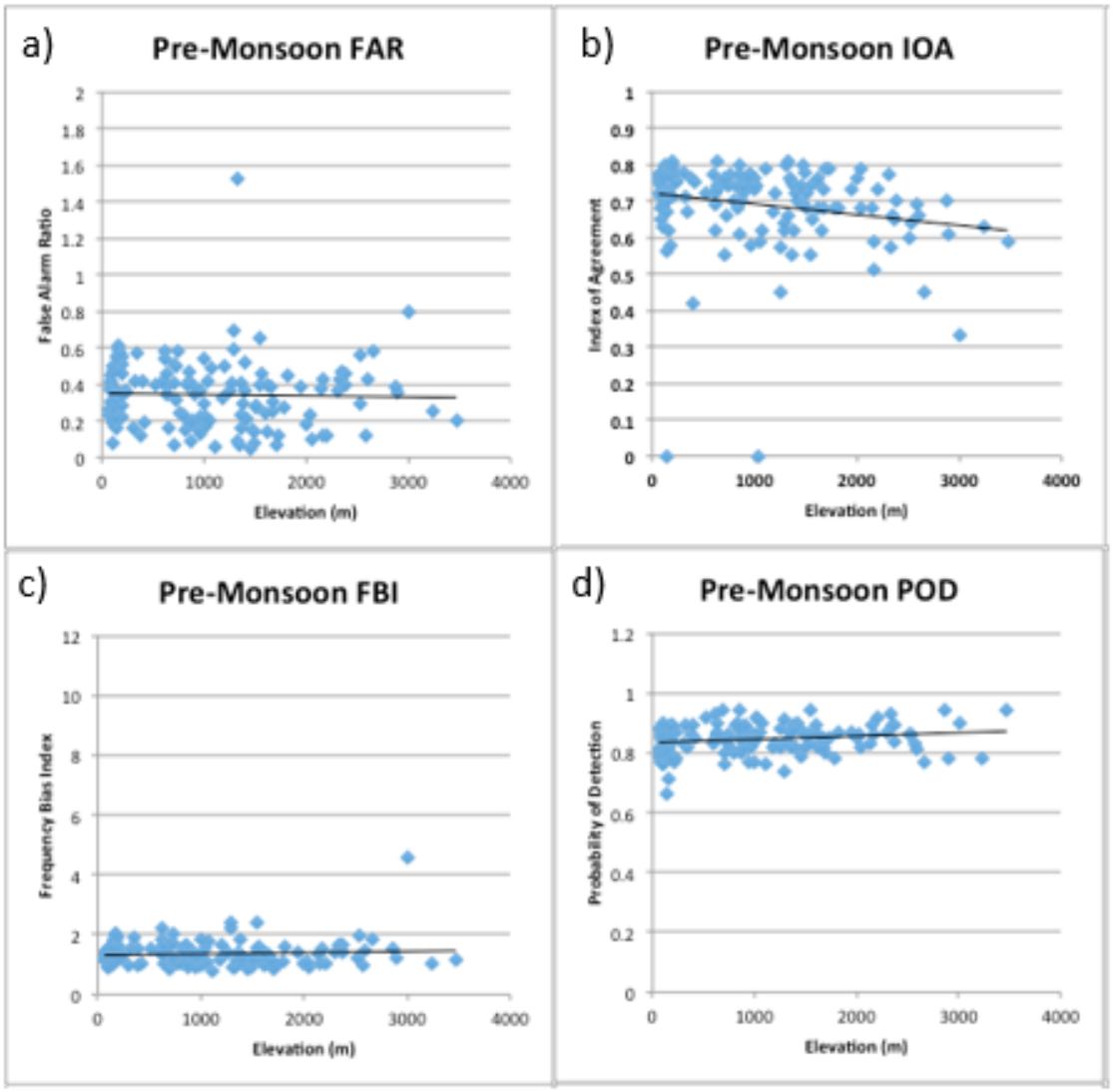

Figure 19. Pre-monsoon seasonal verification statistics compared with elevation. Statistical elements include a) false alarm ratios, b) indices of agreement, c) frequency bias indices, and d) probabilities of detection.

4.3.3 Monsoon Season

The monsoon season, as expected, is characterized by the least amount of spatial variability for each of the four statistical analyses, likely due to the relatively uniform pattern of high precipitation during this season. There are distinct differences in index of agreement values between seasons, with the monsoon season characterized by the greatest overall agreement, followed by the post-monsoon, pre-monsoon, and winter seasons (Table 3). As in the pre-monsoon season the FBI indicates overestimation of precipitation by TRMM for the majority of Nepal, with underestimations indicated for

the grid cells which have the greatest number of precipitation gauges (Figure 20b). The POD for the monsoon season is generally high, due to the increased number of precipitation days during that time of year (Figure 20c). FAR values are smallest during the monsoon season, with moderate to high FAR values evident during the post-monsoon and winter seasons (Table 3). As stated previously, the low FAR values for the monsoon season could relate to the increase in precipitation during this time of the year across Nepal. The influence of elevation during the monsoon season may play a role in the statistically significant IOA and POD. The regression analysis relating elevation to each of these statistical measures indicates a slight negative IOA-elevation relationship and a positive POD-elevation relationship (Figure 21b; Figure 21d).

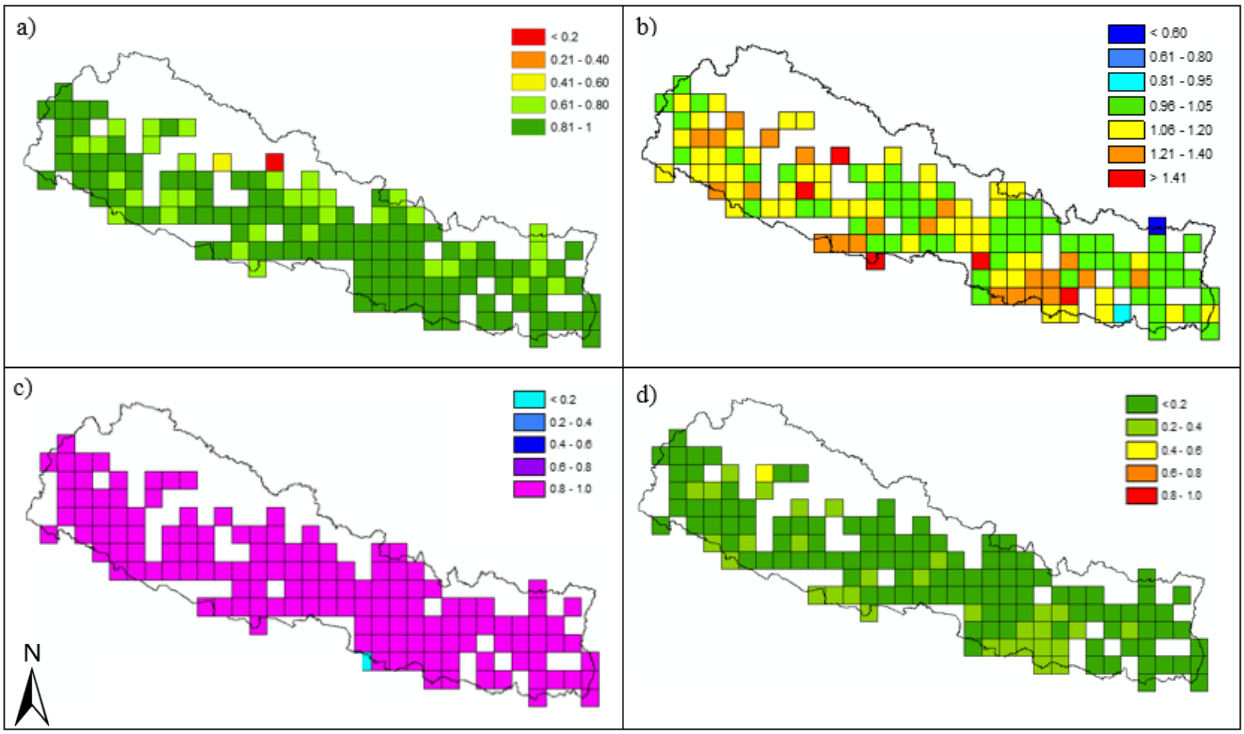

Figure 20. Same as Figure 18, but for the monsoon season.

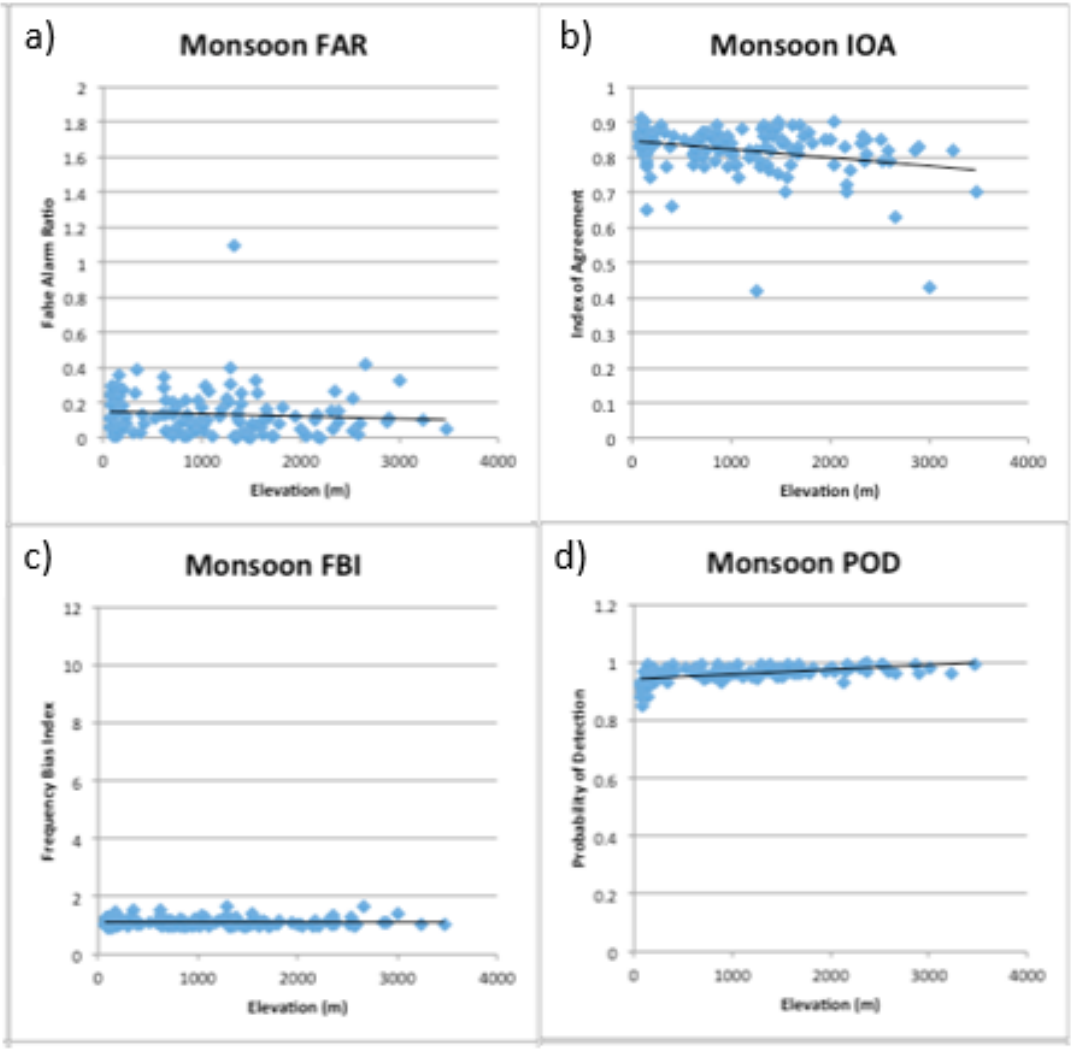

Figure 21. Same as Figure 19, but for the monsoon season.

4.3.4 Post-Monsoon Season

The post-monsoon season, along with the winter season, is characterized by the most spatial variation in the statistical measures across Nepal. The IOA shows relatively high TRMM-gauge agreement through the far eastern, central, and far western regions of Nepal (Figure 22a). The spatial analysis of the FBI (Figure 22b) shows the frequent overestimation during the post-monsoon season, the most of any season (Table 3). The smallest POD values are located across the middle to high mountain regions throughout Nepal, but some of the greatest POD values occur at both low and high elevations (Figure 22c). During the post-monsoon season the FAR is higher across the western half of Nepal, with the smallest FAR occurring across the grid cells with the greatest gauge

densities (Figure 22d). The post-monsoon season is characterized by statistically significant relationships for IOA and FAR as those measures relate to elevation. The statistic-elevation regression analysis for IOA indicates a decrease in IOA with elevation (Figure 23b), while that for FAR indicates an increase in FAR with elevation (Figure 23a).

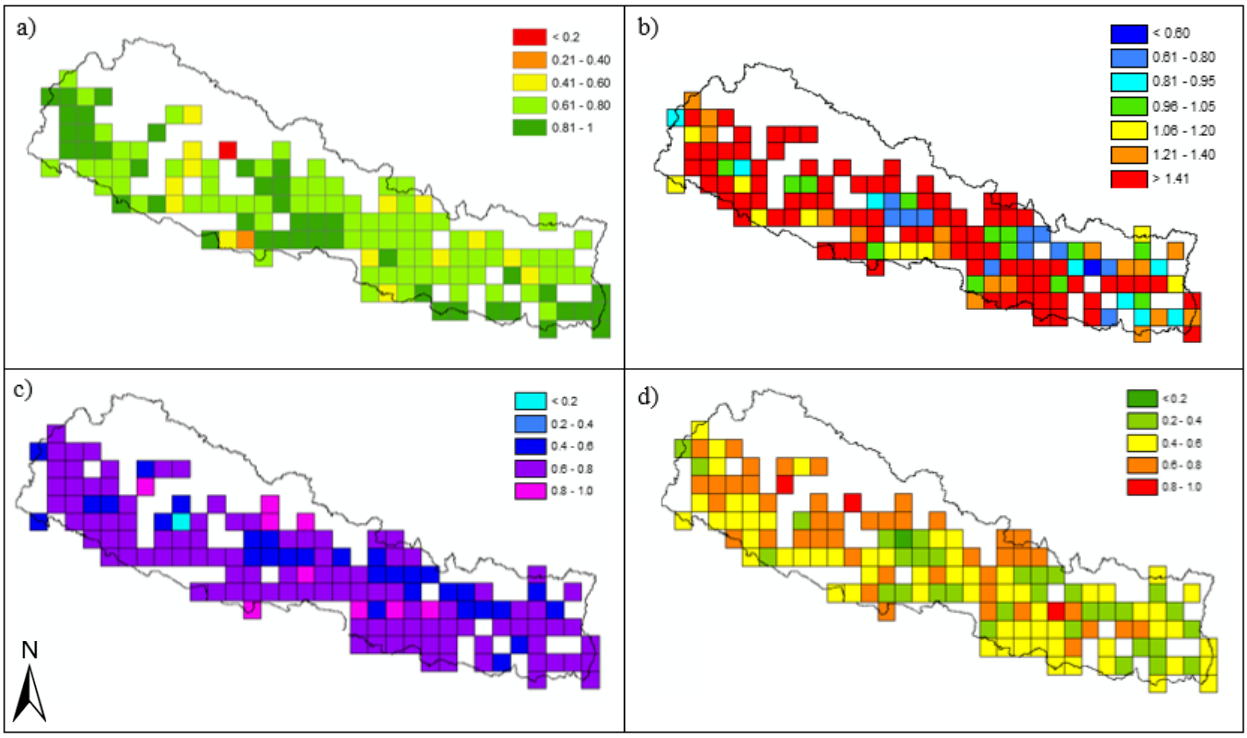

Figure 22. Same as Figure 18, but for the post-monsoon season

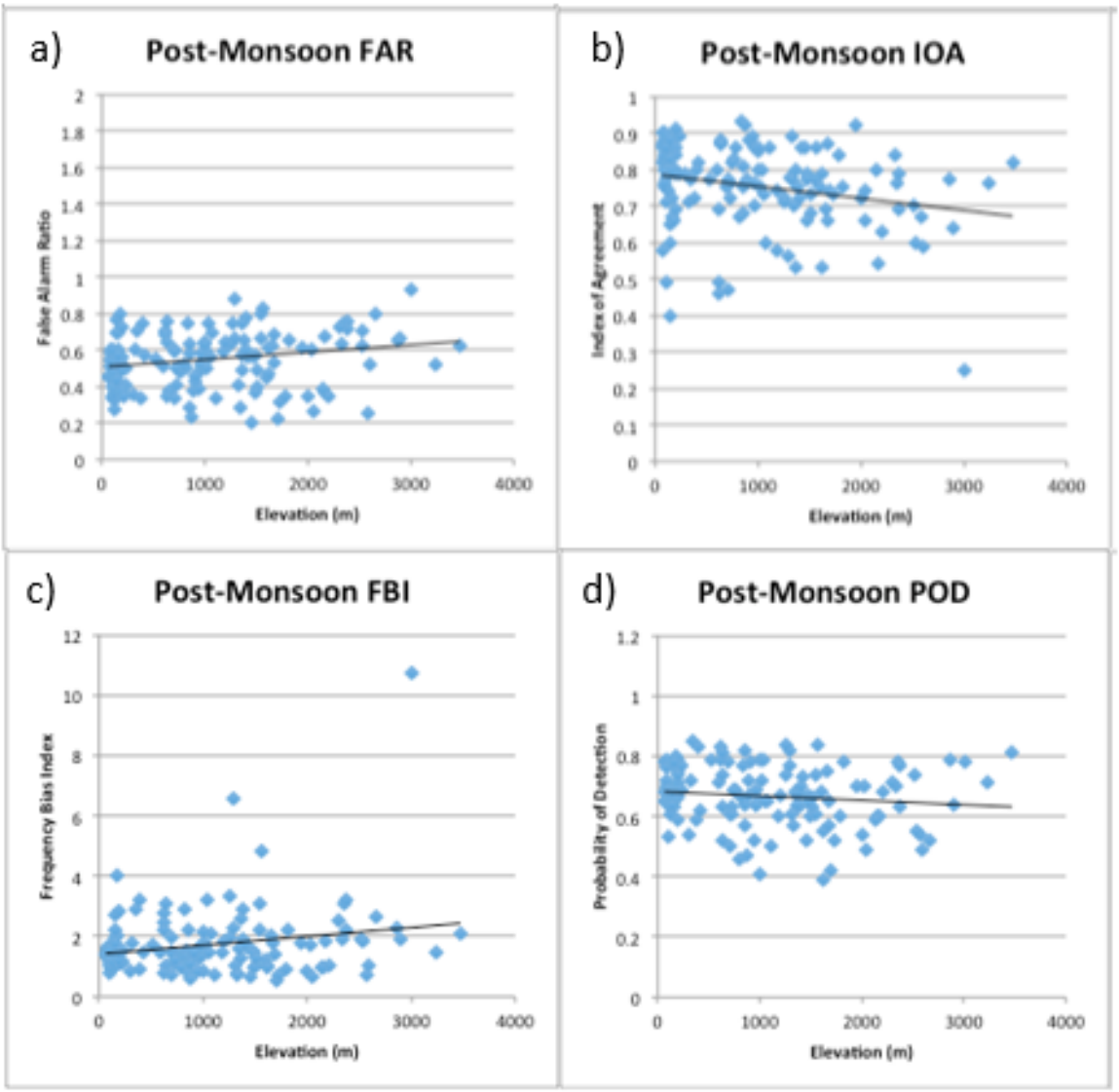

Figure 23. Same as Figure 19, but for the post-monsoon season.

4.3.5 Winter Season

Various issues arise concerning the verification of TRMM during the winter season across Nepal. A lack of knowledge about the types of gauge measuring instruments used in the ground validation dataset leads to the uncertainty of the winter precipitation measured by the Nepalese precipitation gauges. Previous research has concluded that TRMM is a poor estimator of winter precipitation types (Anderman et al. 2011 and Chen et al. 2013). The TRMM validation study conducted by Duncan and Biggs (2012) assessed TRMM's ability to estimate precipitation during the winter season, and observed the greatest correlation of TRMM to their APHRODITE product across

central Nepal. The products produced by TRMM were not designed to be a reliable estimator of winter precipitation, but since the majority of the frozen precipitation occurs at elevations above 3,000 meters and only 3 gauges used in this validation are situated above the threshold elevation, the winter season was analyzed for TRMM verification.

Great spatial variation in the statistical measures of the TRMM-gauge relationship is evident during the winter season, which may be a result of the various precipitation types that occur during this time of year, especially across the higher elevations of Nepal. During the winter season the greatest overestimation occurs across the lowland and high mountain areas (Figure 24b). A pattern can be seen in the spatial distribution of the probability of detection (POD) during the winter season, with higher POD values across the low elevation regions to the south and west, and smaller PODs throughout the middle and high elevations to the north and east (Figure 24c). Statistically significant relationships are found for POD and FAR values with elevation across Nepal during the winter. The regression analyses indicate a decrease in POD and an increase in FAR with elevation (Figure 25a; Figure 25d).

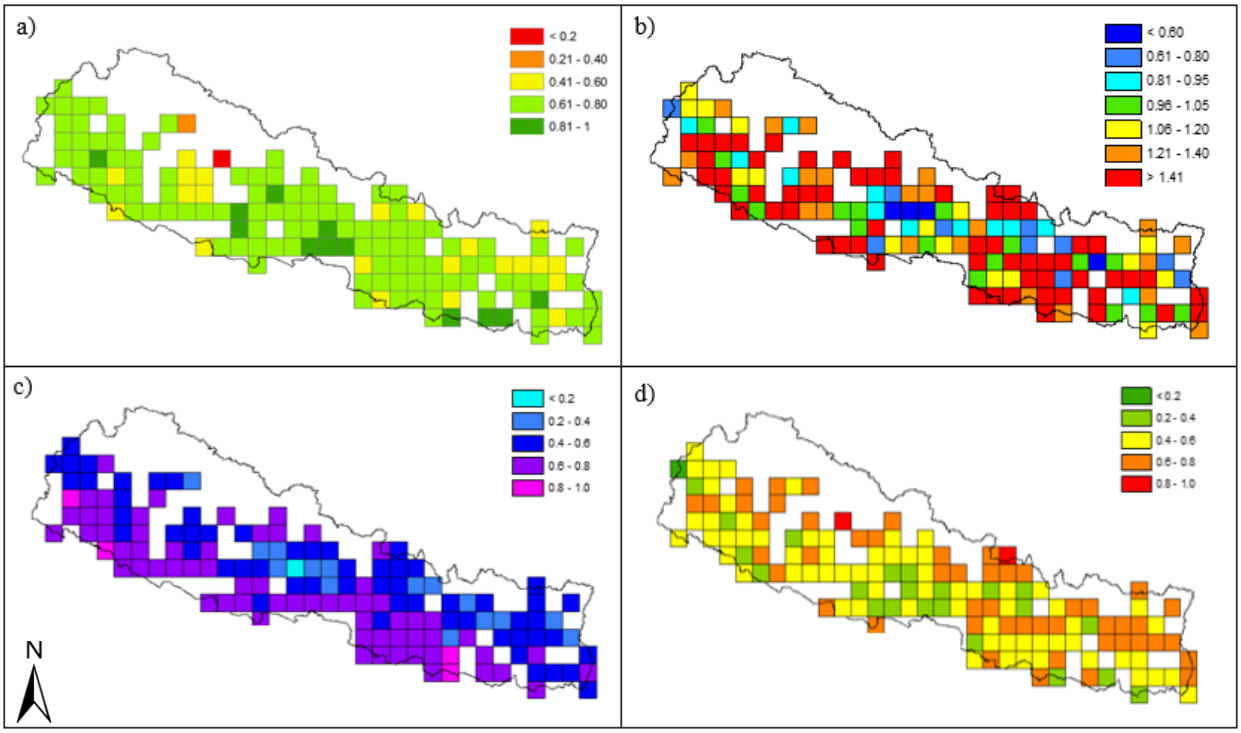

Figure 24. Same as Figure 18, but for the winter season.

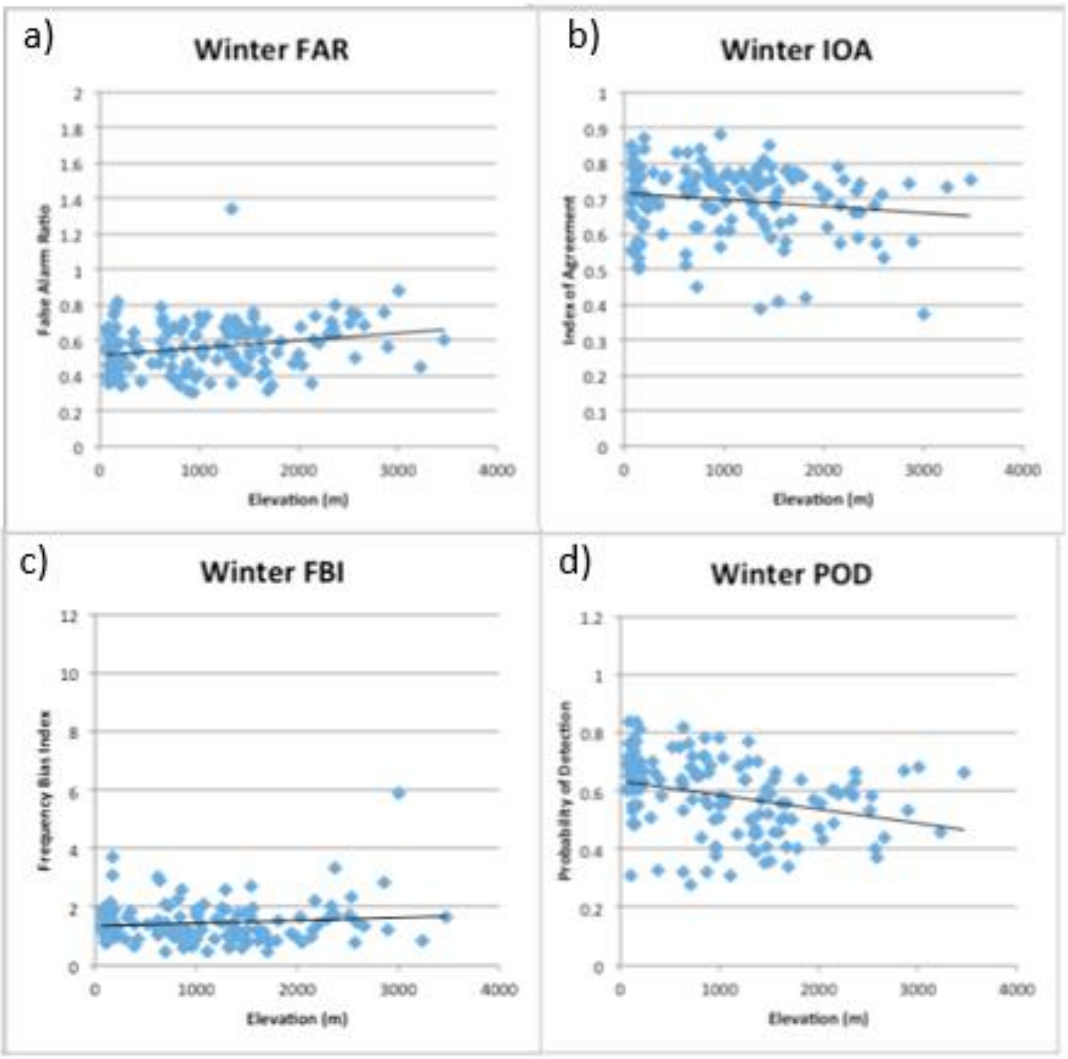

Figure 25. Same as Figure 19, but for the winter season.

Overall the IOA is relatively high across all seasons, which indicates good agreement between TRMM and the precipitation gauge observations throughout the year. Simple regression analyses revealed statistically significant relationships between the statistical elements and elevation. The greatest spatial variation occurred during the winter and post-monsoon seasons, with the monsoon season showing the least variation. The lack of spatial variability in the statistics measured during the summer monsoon may relate to the widespread and frequent precipitation that occurs during that season. The overall indication by the FBI reveals overestimation by TRMM across the majority of the country.

4.3.6 Kathmandu Case Study

A case study of the TRMM grid cell containing the capital city of Kathmandu, Nepal was undertaken to get a more detailed perspective of TRMM performance. This cell contains the greatest number of precipitation gauges, with 13 gauges located within this one grid cell. The average elevation across this grid cell, according to the STRM digital elevation model data, is 1,608 m with a maximum and minimum elevation across the grid cell of 2,748 meters and 1,310 meters. The mean elevation for the 13 gauge locations in this cell is 1,433 meters, with highest and lowest elevations at 1,690 meters and 1,330 meters. The spatial distribution of the stations is also important, if the gauges are clustered around elevations close to the mean grid cell elevation, they would not represent the variation of elevation across the grid cell. The spatial distribution of the precipitation gauges will be noted to better understand the variability in elevation represented by the observations.

4.3.7 Mean Seasonal Precipitation Analysis

To contextualize the case study grid cell, the mean seasonal precipitation values calculated using TRMM and gauge data for Nepal as a whole are compared to those for the Kathmandu grid cell (Figure 26a; Figure 26b). For the pre-monsoon season across the 14-year time period, TRMM overestimated precipitation according to the country-wide analysis as well as across the Kathmandu grid cell. TRMM indicates a significant overestimation during the summer monsoon season across the Kathmandu cell, while when considering all cells, TRMM data underestimate precipitation during that season. The opposite is true for the post-monsoon season, where underestimates were made by TRMM for the country as a whole, but overestimation was made across the individual Kathmandu cell. The only season where the TRMM data consistently underestimated was during winter. This illustrates that the statistics for the country-wide analysis do not necessarily translate directly to any individual TRMM grid cell across Nepal. In reality precipitation is generally highly variable across the study region, therefore it is inaccurate to assume that precipitation is uniform across a grid cell. This is a caveat when interpreting the statistics for the country as a whole, as the point-specific gauge may not reflect the precipitation observed across the entirety of the cell. This stipulation places

the TRMM satellite estimate at a disadvantage when calculating the statistics, especially for grid cells which contain very few precipitation gauges.

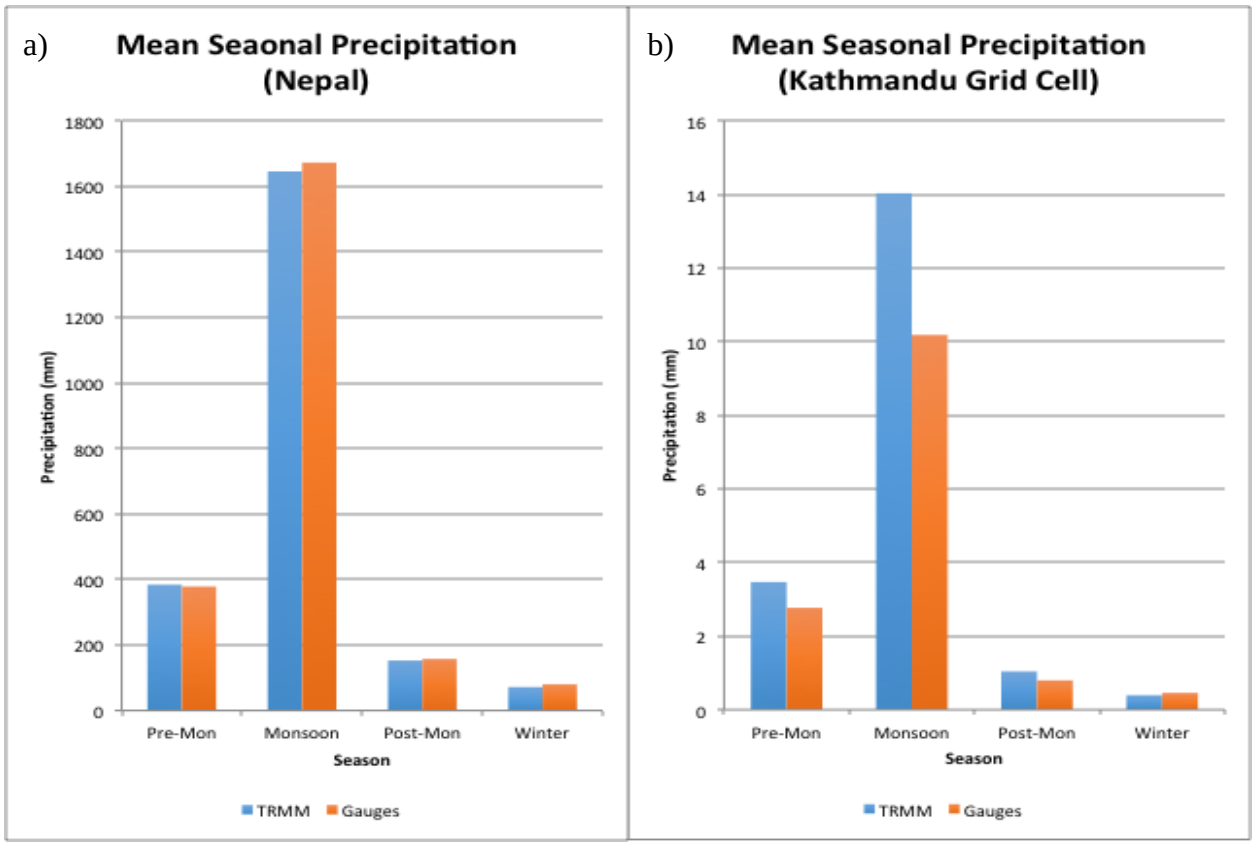

Figure 26. Mean seasonal precipitation for all TRMM grid cells containing gauges across Nepal (a) and mean seasonal comparison of TRMM and gauge estimates across the Kathmandu grid cell (b)

4.3.8 Extreme Precipitation Analysis

In order to get an idea of how accurate TRMM estimates are during high precipitation events within the case study grid cell, the ten greatest precipitation days according to the gauges and the TRMM estimates were analyzed. The 10 precipitation days with the greatest precipitation amount, as determined first by the mean precipitation from the 13 gauges within the TRMM cell, were identified for each season. The same analysis was performed for the 10 greatest TRMM estimated precipitation days for the Kathmandu grid cell. The TRMM-estimated precipitation amount was compared to the average, maximum, minimum precipitation and the standard deviation of the 13 gauges (Figure 27; Figure 28) to depict within-cell variability.

During the pre-monsoon season, TRMM underestimated the gauge average on all but one day, where it overestimated by 7.8 mm (Figure 27a). TRMM matched more closely with the minimum rather than the average gauge precipitation for 8 out of the 10 days. This could indicate that TRMM tends to underestimate high precipitation events, especially during the pre-monsoon season, but more analysis would need to be completed before that assumption could be validated definitively.

When examining the data for the summer monsoon, TRMM overestimated precipitation during one-half of the ten high intensity precipitation days (Figure 27b). During those five days the TRMM estimate differs by an average of 9.6 mm from the maximum gauge precipitation. Since TRMM overestimated and underestimated an equal number of days, TRMM data are not biased high or low during the monsoon season during extreme precipitation events during the monsoon season according to this analysis.

For the post-monsoon season, TRMM overestimated the average station precipitation on two of the ten days (Figure 27c). During 9 of the 10 days, at least one gauge reported zero precipitation. This indicates that for the post-monsoon season high intensity precipitation days, the heavy precipitation fell in one portion of the grid cell area rather than uniformly across the cell. TRMM did not detect any precipitation for the greatest intensity precipitation day during this season.

Kathmandu experiences the least amount of precipitation during the winter season. Snowfall is rare for the city of Kathmandu and the surrounding valleys. According to the Department of Meteorology of Nepal snowfall has only occurred twice during the TRMM verification study period in Kathmandu; February 2007 and January 2011. The snowfall that occurred in February of 2007 was the first snowfall recorded in Kathmandu in 63 years (Department of Meteorology of Nepal). For the winter season, the TRMM data reveal zero precipitation for seven of the ten high precipitation days (Figure 27d). During each of those days there was at least one gauge that reported zero precipitation, but the precipitation that was recorded within that entire cell averaged between 18 and 25 mm. This absence of detection by TRMM could be in part due to the spatial distribution of the gauges in relation to the Kathmandu valley region. These Figures show that TRMM performs differently during high intensity precipitation events

across all four seasons, and no one TRMM correction factor can be applied to all high precipitation events.

a)

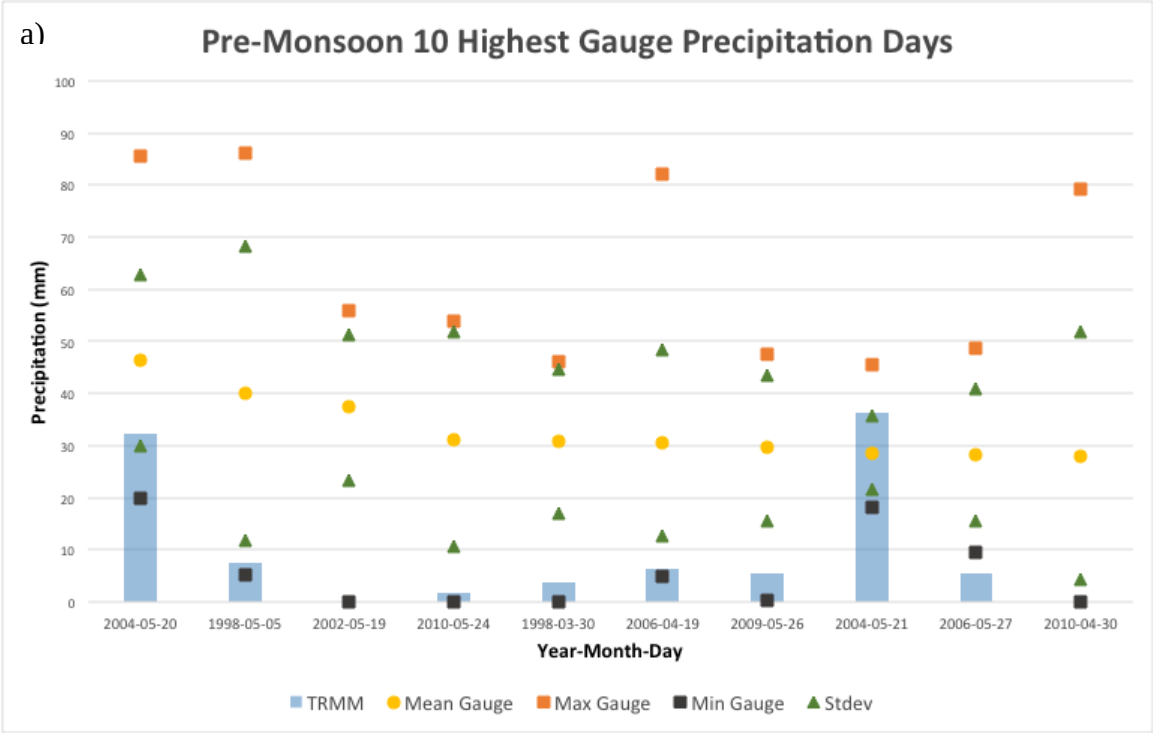

b)

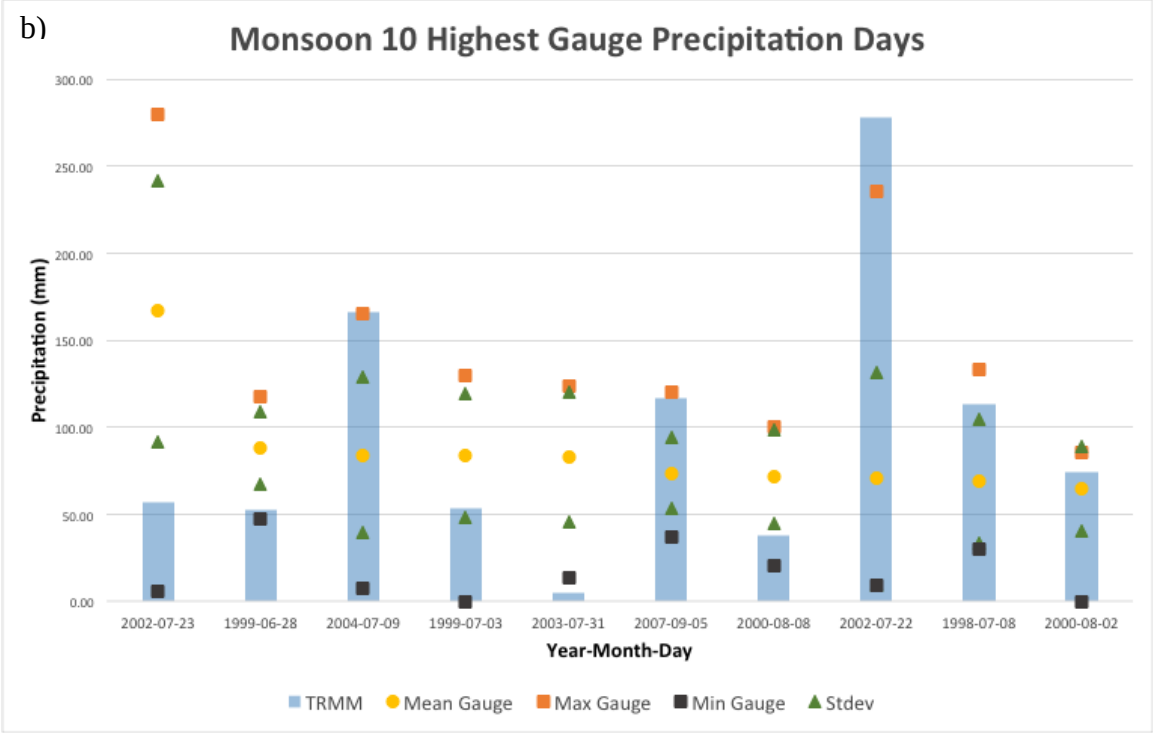
Monsoon 10 Highest Gauge Precipitation Days
Precipitation (mm)
300.00
250.00
200.00
150.00
100.00
50.00
0.00
2002-07-23
1999-06-28
2004-07-09
1999-07-03
2003-07-31
2007-09-05
2000-08-08
2002-07-22
1998-07-08
2000-08-02
Year-Month-Day
TRMM
Mean Gauge
Max Gauge
Min Gauge
Stdev

c)

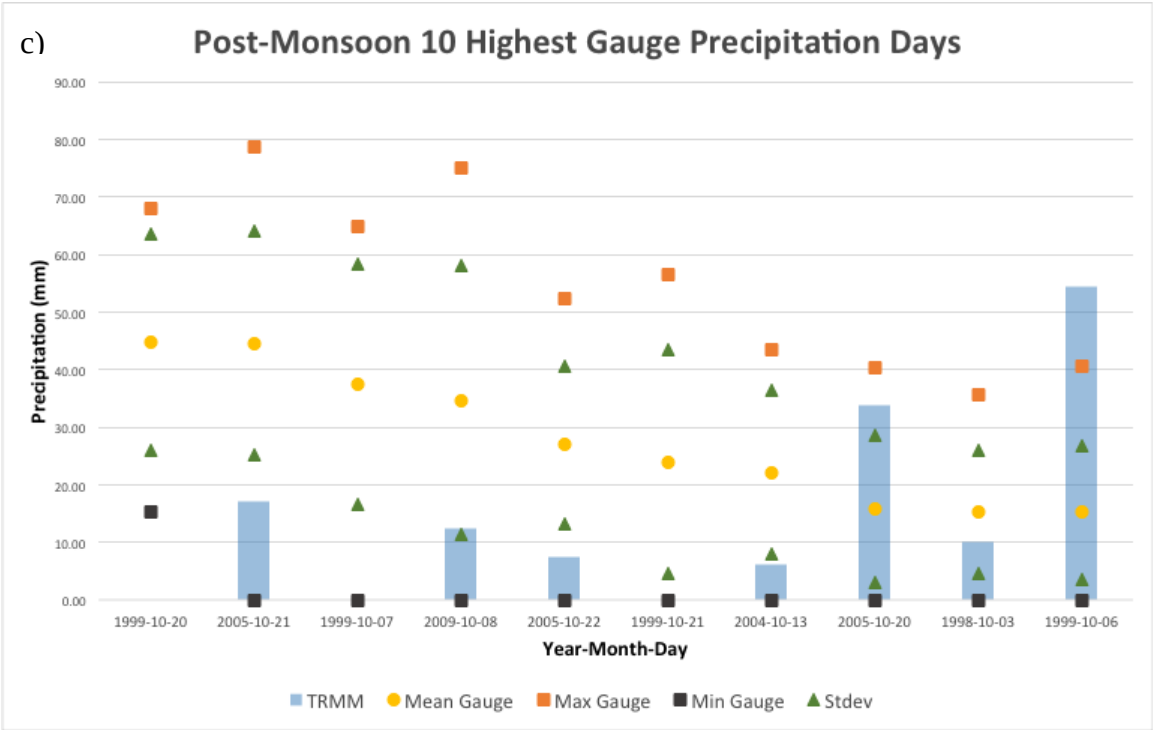
Post-Monsoon 10 Highest Gauge Precipitation Days
Precipitation (mm)
90.00
80.00
70.00
60.00
50.00
40.00
30.00
20.00
10.00
0.00
1999-10-20
2005-10-21
1999-10-07
2009-10-08
2005-10-22
1999-10-21
2004-10-13
2005-10-20
1998-10-03
1999-10-06
Year-Month-Day
TRMM
Mean Gauge
Max Gauge
Min Gauge
Stdev

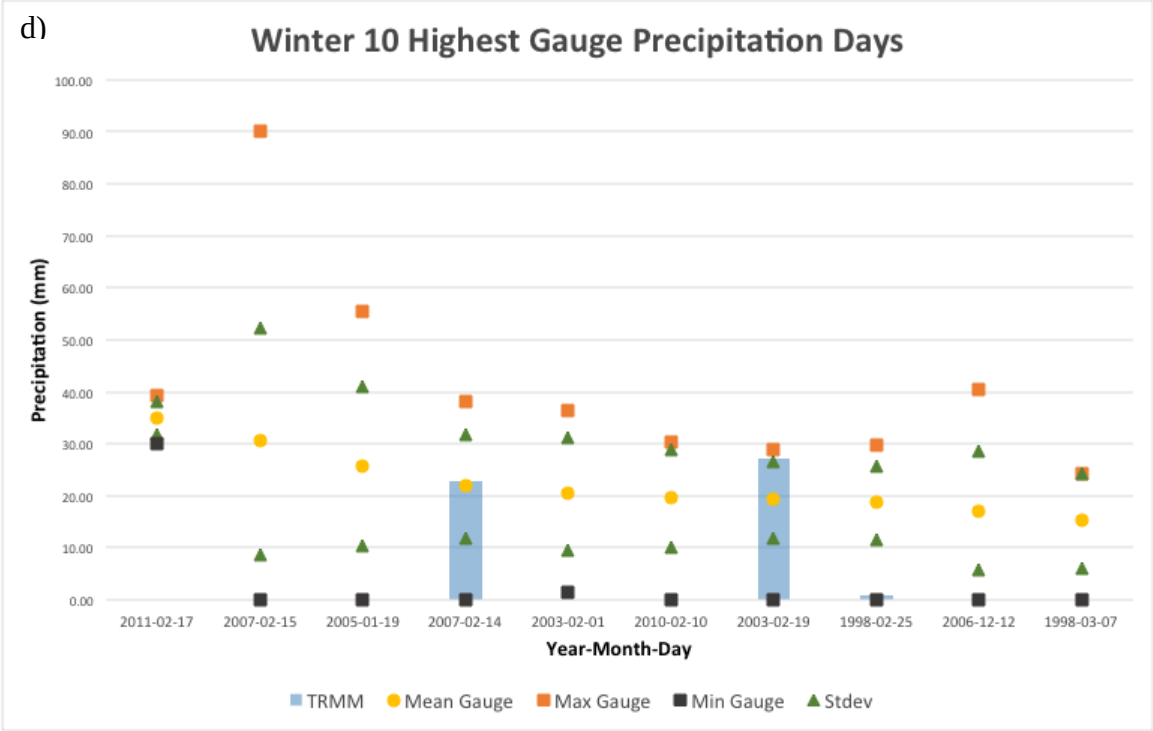

Figure 27. Statistics for the ten largest precipitation days based on the average station precipitation across the Kathmandu grid cell for each season and the TRMM estimated precipitation for that day. The four seasons are shown: a) pre-monsoon, b) monsoon, c) post-monsoon, and d) winter.

The extreme daily precipitation analyses were repeated, but for the ten greatest precipitation days as estimated by TRMM for each of the four Nepalese seasons (Figure 28a; Figure 28b; Figure 28c; Figure 28d). For all of these instances across every season TRMM overestimated the average precipitation reported by the gauges across the grid cell. The best estimation of the average precipitation by TRMM during the monsoon season still indicated a large difference of 43 mm between the average station amount and TRMM. During the monsoon and post-monsoon seasons TRMM overestimated the maximum precipitation observation on 8 of the 10 days. On at least 2 of the high precipitation days across each season, TRMM estimated the daily precipitation amount to be between the average and the maximum observed precipitation. In summary, an extreme precipitation event as indicated by TRMM ideally should first be verified by ground reports, since TRMM has a tendency to overestimate the extreme events across every season.

a)

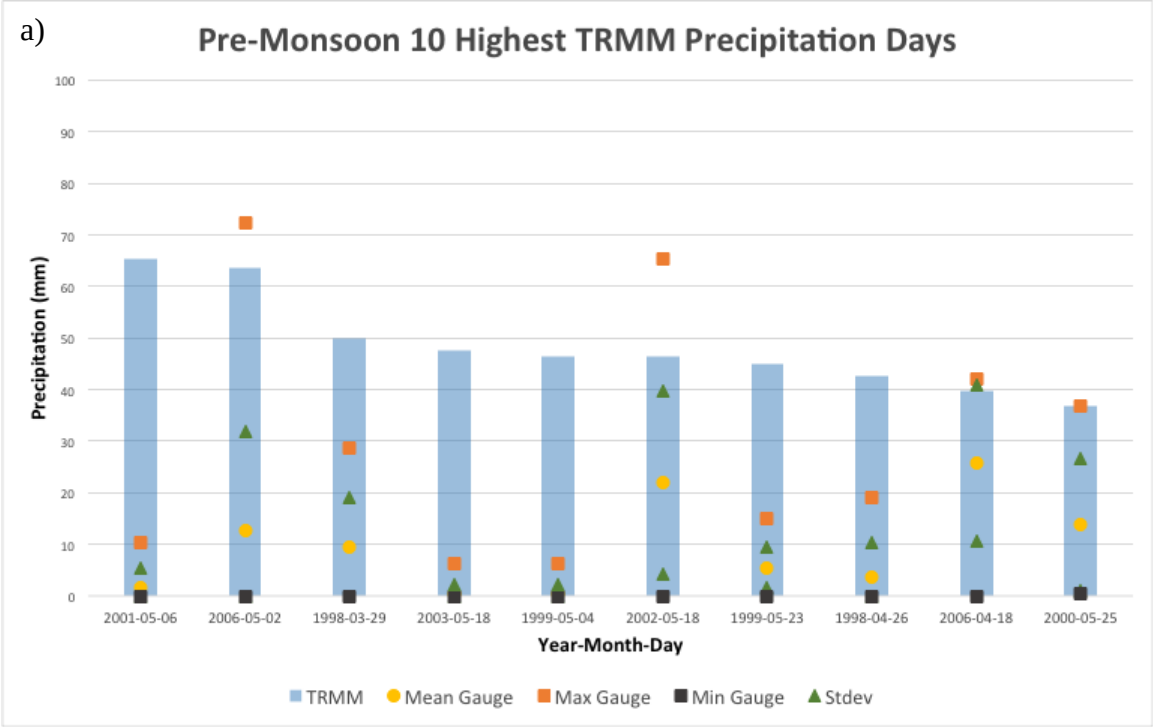
Pre-Monsoon 10 Highest TRMM Precipitation Days
Precipitation (mm)
100
90
80
70
60
50
40
30
20
10
0
2001-05-06
2006-05-02
1998-03-29
2003-05-18
1999-05-04
2002-05-18
1999-05-23
1998-04-26
2006-04-18
2000-05-25
Year-Month-Day
TRMM
Mean Gauge
Max Gauge
Min Gauge
Stdev

b)

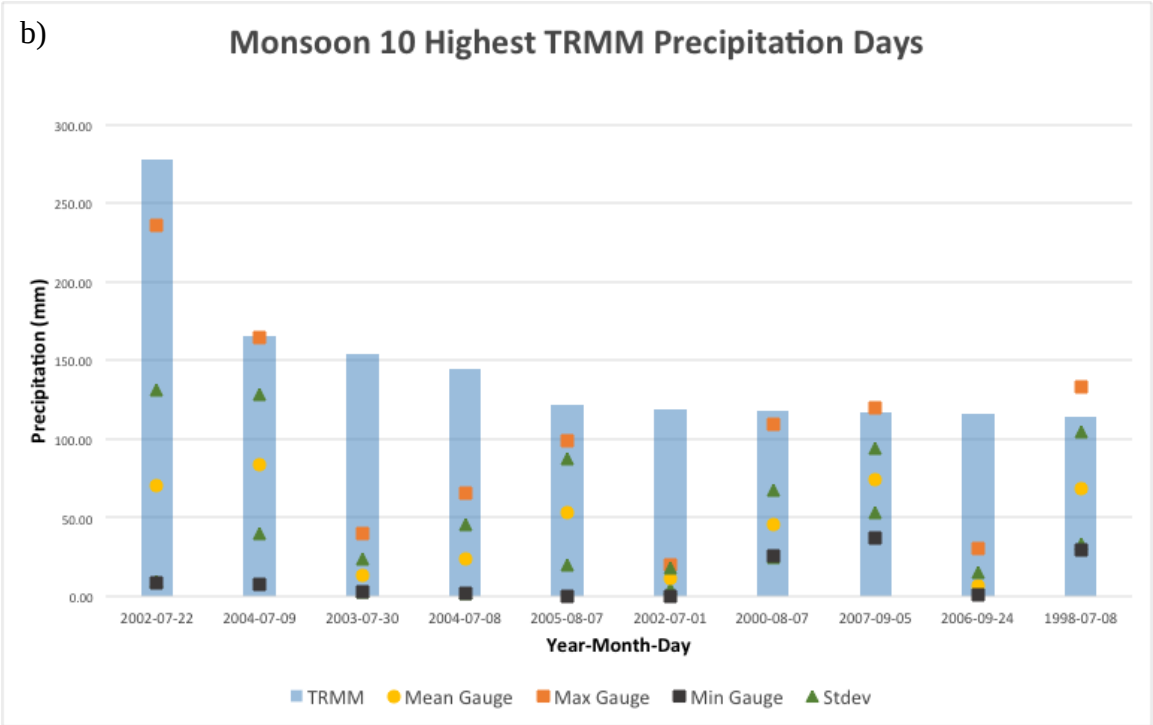
Monsoon 10 Highest TRMM Precipitation Days
Precipitation (mm)
300.00
250.00
200.00
150.00
100.00
50.00
0.00
2002-07-22
2004-07-09
2003-07-30
2004-07-08
2005-08-07
2002-07-01
2000-08-07
2007-09-05
2006-09-24
1998-07-08
Year-Month-Day
TRMM
Mean Gauge
Max Gauge
Min Gauge
Stdev

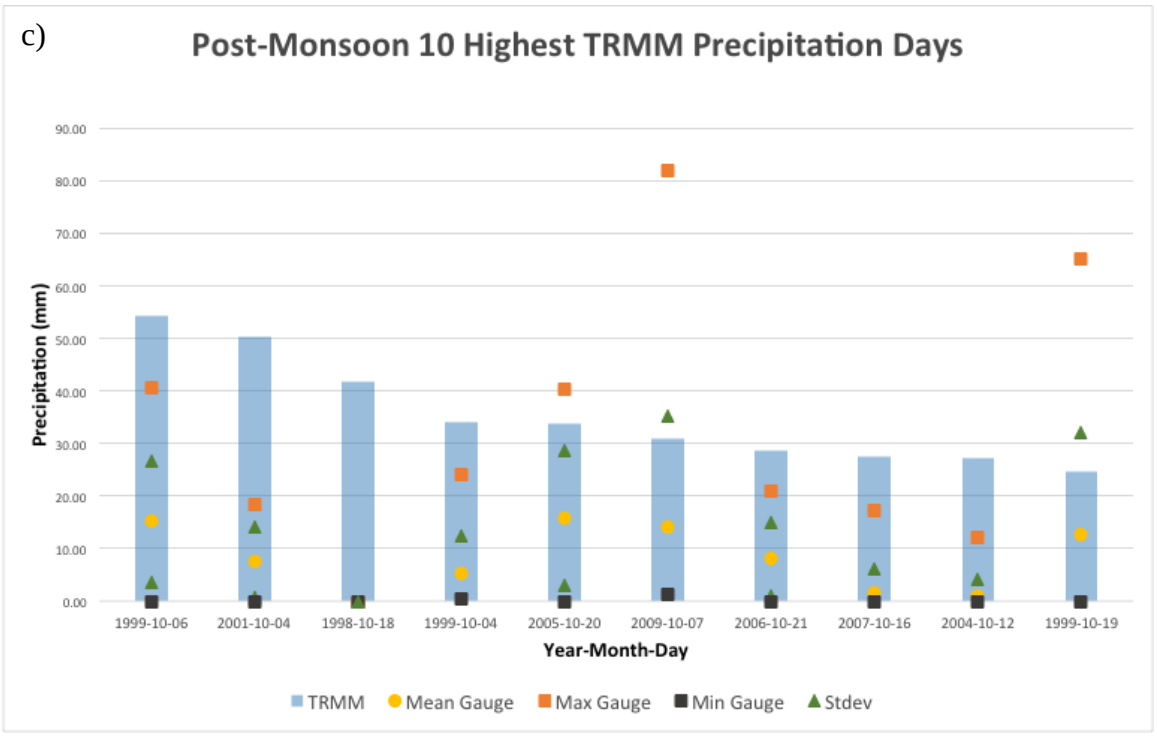

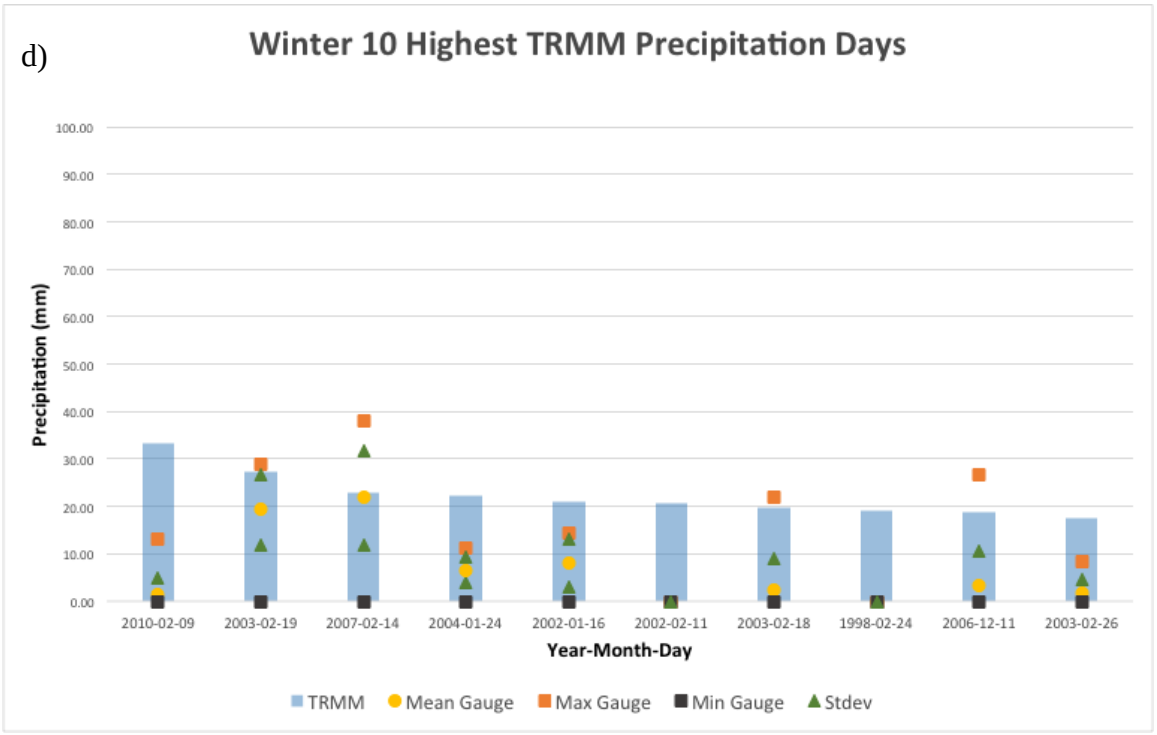

Figure 28. The ten largest precipitation days based on the TRMM estimated daily precipitation across the Kathmandu grid cell for each season and the statistics for the

precipitation gauge observations. The four seasons are shown: a) pre-monsoon, b) monsoon, c) post-monsoon, and d) winter.

The scatter plots shown in Figure 29 illustrate TRMM data versus the average daily gauge precipitation for the Kathmandu grid cell for each of the four seasons. The greatest agreement between TRMM and the daily gauge observations occurs during the summer monsoon season, followed by the post-monsoon, winter and pre-monsoon seasons. The largest difference between TRMM and gauge precipitation occurs during the winter, which aligns with the statistical analysis presented earlier (Table 3). TRMM generally underestimates precipitation for the case study grid cell for each of the four seasons. The individual cell used in this case study shows somewhat different patterns of agreement between TRMM and the precipitation gauges than for the analysis using data from across Nepal, which further shows the overall seasonal patterns cannot be assumed to be that of each individual grid cell. Additional investigation is needed to pinpoint the bias behavior of TRMM.

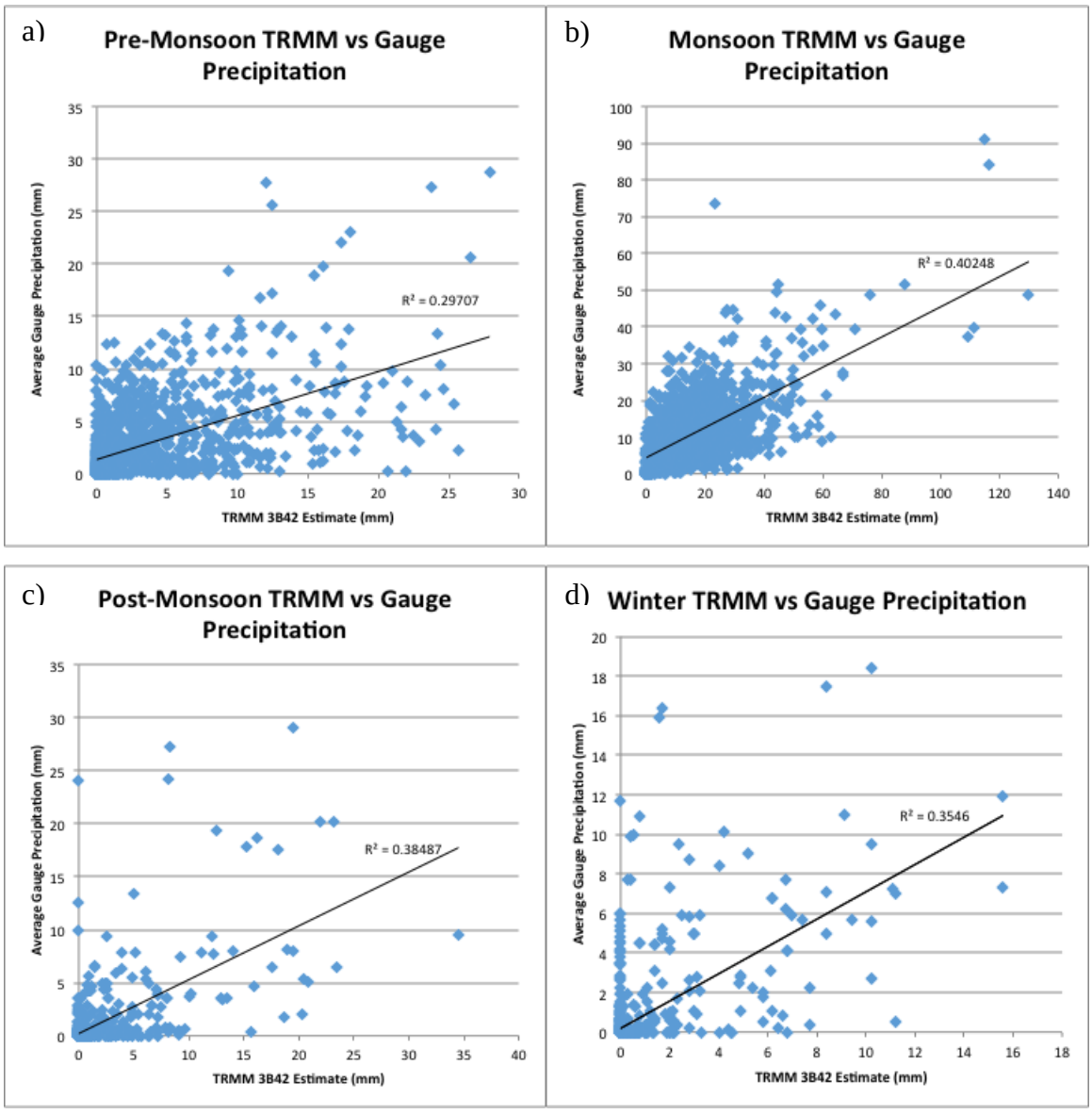

Figure 29. Scatter plot of TRMM 3B42 versus daily mean gauge precipitation for the Kathmandu grid cell for each season a) pre-monsoon, b) monsoon, c) post-monsoon and d) winter.

The bias of TRMM daily precipitation is investigated using the TRMM data for the period of study for all 13 precipitation gauges within the Kathmandu grid cell (Figure 30). A bias analysis assesses the average difference between the satellite estimation and the gauge precipitation amount. A bias value greater than 0 indicates an overestimation with negative values showing an average underestimation by TRMM. This bias analysis indicates mean overestimation of precipitation below 10 mm day^{-1}, with overestimation occurring at rates greater than this threshold. The bias of TRMM shows the same overall

pattern for each of the 13 gauges. The greatest disparity occurs at the lowest precipitation rates, from 0.1 mm to 0.5 mm day^{-1}, with increasing agreement coinciding with increasing precipitation rates. This bias of TRMM across Nepal shows the same general pattern, but with a higher precipitation intensity threshold for overestimation, as did the bias of TRMM across La Paz, Bolivia and Cuzco, Peru as reported by Scheel et al. (2011). Scheel et al. displayed an underestimation of TRMM starting at 2 mm day^{-1} while the analysis across Nepal yielded underestimation beginning at 10 mm day^{-1}. From this, TRMM is noted to generally overestimate during daily precipitation events where less than 10 mm are observed, while underestimating daily precipitation amounts greater than 20 mm.

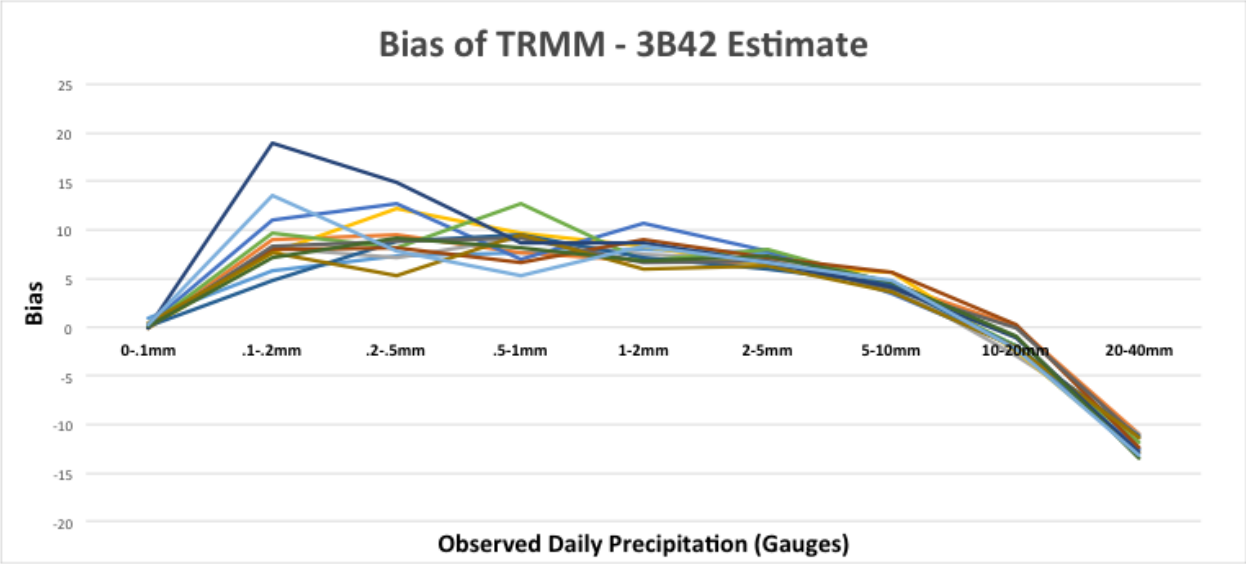

Figure 30. Bias of TRMM 3B42 versus observed gauge daily precipitation for each of the 13 stations within the Kathmandu TRMM grid cell (1998-2011).

The investigation of the Kathmandu grid cell was completed to give a more detailed look at the accuracy of TRMM. This case study detailed the precipitation variation that can occur across a TRMM grid cell. The most telling of the statistical analyses for the Kathmandu grid cell is the bias investigation of the TRMM 3B42 product, uncovering the threshold of 10 – 20mm of precipitation for the overestimation of TRMM. The investigation of extreme precipitation events indicated that extreme precipitation as indicated by TRMM is likely an overestimation, no matter the season.

Overall the TRMM product showed good agreement with the ground observations for the areas surrounding Kathmandu.

Chapter 5

Conclusion

This thesis presented a validation assessment of TRMM data across the south Asian country of Nepal. The results offer guidance to users that struggle to determine if the data are reliable enough for use in historical or operational assessments, especially during the hydrologically critical monsoon season.

A 30-year climatology was first constructed using 210 Nepalese precipitation gauges in order to build a foundation for the TRMM validation assessment. The TRMM 3B42 satellite product was assessed against the historical observations of 141 Nepalese precipitation gauges on a point-to-grid cell basis. The spatial and temporal relationships between TRMM estimates and gauge data were assessed using an array of evaluation statistics generated for each precipitation-defined season. The TRMM estimations were assessed on monthly, seasonal, and annual time scales in order to achieve a broad assessment of TRMM accuracy using 3-day running means of precipitation across Nepal. The analysis of the TRMM data at its original resolution focuses on the quality of the 3B42 daily accumulated precipitation as compared to the Nepalese rain gauge network. A case study was performed on the grid cell containing the most precipitation gauges in order to achieve a better understanding of TRMM accuracy around the capital city of Kathmandu, Nepal.

The climatological examination concluded that Nepal receives close to 80% of its annual precipitation during the monsoon season, which supports the previous study completed by (Kansakar et al. 2004). Nepal experiences the greatest precipitation intensity and frequency during this season as well. The analysis revealed increased mean annual precipitation across the northwestern portion of Nepal during the winter season as first identified by Ichiyanagi et al. (2007). During the transitional seasons, pre-monsoon and post-monsoon, the greatest precipitation intensity and frequency occurs across the far southeastern regions of Nepal due to the summer monsoonal flow influence.

The verification aspect of this study answered the call for additional satellite derived precipitation validation across the Himalaya Mountain region. The TRMM 3B42 V7 daily precipitation product performs differently across all four of the precipitation

driven seasons of Nepal. TRMM underestimation of daily precipitation during the monsoon season supports the findings of Hazarika et al. (2007), though this contradicts the overestimation during the monsoon season as indicated by Duncan and Biggs (2012). Duncan and Biggs (2012) also indicated the largest error of TRMM occurred during the monsoon season, which is supported by the large RMSE value calculated in this research. The performance of TRMM indicated an overestimation during both the post-monsoon and winter seasons, when dry air dominates the climate, while underestimation occurred during the pre-monsoon and monsoon seasons, when moist air and increased precipitation overtakes the region. Dorninger et al. (2008) indicated increased accuracy of TRMM across flat terrain, which was found to be true during all four Nepalese seasons by a decreasing index of agreement with elevation.

According to the Kathmandu case study results, TRMM performs best during light (10 – 20 mm) rainfall events, which supports the results of Liao and Meneghini (2009). In turn, the case study revealed TRMM's bias to underestimate periods of moderate to heavy (> 40 mm) precipitation, contradicting the early findings of Barros et al. (2000), but supporting those of Han (2011). Daily precipitation that measures less than 10 mm was historically overestimated by TRMM for the case study grid cell, which supports the claim by Han (2011) that TRMM overestimates minor rainfall events.

The conclusions from this thesis are potentially important for those using historical TRMM data in scientific study and for those operationally using satellite-derived products in general. Since the TRMM satellite is quickly approaching the end of its life, this verification analysis would be of primary use as a guide for assessing and refining other satellite derived precipitation products, such as CMORPH and the newly launched GPM satellite. A greater understanding of the accuracy of satellite derived precipitation products could lead to algorithm improvement, which will in turn help efforts to protect life and property from precipitation initiated disasters, especially across rural regions and areas of complex terrain.

References

Agrawala, Shardul, et al. "Development and climate change in Nepal: Focus on water resources and hydropower." *Environment Directorate and Development Cooperation Directorate, Organisation for Economic Cooperation and Development (OECD), Paris* (2003).

Andermann, Cristoff et al. "Evaluation of precipitation data sets along the Himalayan front." *Geochemistry, Geophysics, Geosystems* 12.7 (2011).

Artan, Guleid, et al. "Adequacy of satellite derived rainfall data for stream flow modeling." *Natural Hazards* 43.2 (2007): 167-185.

Barros, Ana P et al. "A Study of the 1999 Monsoon Rainfall in a Mountainous Region in Central Nepal using TRMM Products and Rain Gauge Observations." *Geophysical Research Letters* 27 (2000): 3683-3686.

Barros, Ana P and Timothy J. Lang. "Monitoring the Monsoon in the Himalayas: Observations in Central Nepal June 2001." *Monthly Weather* 131 (2003): 1408.

Chen, Yingjun, et al. "Evaluation of TRMM 3B42 precipitation estimates of tropical cyclone rainfall using PACRAIN data." *Journal of Geophysical Research: Atmospheres* 118.5 (2013): 2184-2196.

Dorninger, Manfred et al. "On the interpolation of precipitation data over complex terrain." *Meteorology and Atmospheric Physics*101.3-4 (2008): 175-189.

Duncan, John M.A. and Eloise M. Biggs. "Assessing the Accuracy and Applied use of Satellite Derived Precipitation Estimates over Nepal." *Applied Geography* 34 (2012): 626-638.

Goodison, H.L. Ferguson, G.A. McKay. "Measurement and data analysis." *The Snow Handbook* Pergamon Press (1981): 191–23

Han, Woo Suk et al. "Assessment of Satellite-based Rainfall Estimates in Urban Areas in Different Geographic and Climatic Regions." *Natural Hazards* 56 (2011): 733-747.

Hanson, Brian, et al. "Vector correlation: review, exposition, and geographic application." *Annals of the Association of American Geographers* 82.1 (1992): 103-116.

Hazarika, M. K., et al. "Statistical approach to discharge prediction for flood forecasts using TRMM data." *Proceedings of the 5th Annual Mekong Flood Forum, Ho Chi Minh City, Vietnam*. 2007.

Hirpa, Feyera A. et al. “Evaluation of High-Resolution Satellite Precipitation Products over Very Complex Terrain in Ethiopia.” *Journal of Applied Meteorology and Climatology* 49 (2010): 1044-1051.

Huffman, George J. and David T. Bolvin. "TRMM and other data precipitation data set documentation." *NASA, Greenbelt, USA* (2013): 1-40.

Ichiyanagi, Kimpei, et al. "Precipitation in Nepal between 1987 and 1996."*International Journal of Climatology* 27.13 (2007): 1753-1762.

Islam, Nazrul et al. “Calibration of TRMM Derived Rainfall Over Nepal During 1998-2007.” *The Open Atmospheric Science Journal* (2010): 12-23.

Kansakar, Sunil et al. “Spatial Pattern in the Precipitation Regime of Nepal.” *International Journal of Climatology* 24 (2004): 1645-1659.

Krakauer, Nir Y. et al. “Evaluating Satellite Products for Precipitation Estimation in Mountain Regions: A Case Study for Nepal.” *Remote Sensing* 5 (2013) 4107-4123.

Kummerow, Christian, et al. "The tropical rainfall measuring mission (TRMM) sensor package." *Journal of Atmospheric and Oceanic Technology* 15.3 (1998): 809-817.

Liao, L. and Meneghini, R. “Validation of TRMM Precipitation Radar through Comparison of Its Multiyear Measurements with Ground-Based Radar”, *Journal of Applied Meteorology and Climatology*, 48, 804–817, doi:10.1175/2008jamc1974.1, 2009.

McDowell, G. et al. “Climate-related Hydrological Change and Human Vulnerability in Remote Mountain Regions: A Case Study from Khumbu, Nepal.” *Regional Environmental Change* (2013): 299-310.

Moriasi, D. N., et al. "Model evaluation guidelines for systematic quantification of accuracy in watershed simulations." *Transations of the American Society of Agricultrual and Biological Engineers* 50.3 (2007): 885-900.

Myrick, David T. et al. "Local adjustment of the background error correlation for surface analyses over complex terrain." *Weather and forecasting* 20.2 (2005): 149-160.

Nešpor, Vladislav, and Boris Sevruk. "Estimation of wind-induced error of rainfall gauge measurements using a numerical simulation." *Journal of Atmospheric and Oceanic Technology* 16.4 (1999): 450-464.

Panthi, Jeeban, et al. "Spatial and Temporal Variability of Rainfall in the Gandaki River Basin of Nepal Himalaya." *Climate* 3.1 (2015): 210-226.

Sevruk, B. “Correction of precipitation measurements.” Proc. Workshop on the Correction of Precipitation Measurements, Zurich, Switzerland, WMO/IAHS/ETH, (1985): 13–23.

Sharma, R.R. et al. “Applicability of Tropical Rainfall Measuring Mission to Predict Foods on the Bagmati River.” *Journal of Hydrology and Meteorol*ogy 4 (2007): 1–15.

Shin, DB et al. “Comparison of the monthly precipitation derived from the TRMM satellite.” *Geophysical Research Letters* 28.5 (2001):795–798

Shrestha, Arun B. et al. "Maximum temperature trends in the Himalaya and its vicinity: An analysis based on temperature records from Nepal for the period 1971-94." *Journal of Climate* 12.9 (1999): 2775-2786.

Shrestha, MS et al. “Using satellite-based rainfall estimates for streamflow modeling: Bagmati Basin.” *Journal of Flood Risk Management* 1.2 (2008):89–99.

Shrestha, Anushiya and Sada Rajesh. “Evaluating the changes in climate and its implications on peri-urban agriculture”. *Research Journal of Agriculture Science and Soil Sciences Vol.* 1.4 (2013): 048-057

Subimal Ghosh et al. “Trend analysis of Indian summer monsoon rainfall at different spatial scales.” *Atmospheric Science Letters.* 10 (2009): 285-290

Ueno, Kenichi, et al. "Meteorological observations during 1994-2000 at the automatic weather station (GEN-AWS) in Khumbu region, Nepal Himalayas." *Bulletin of glaciological research.* 18 (2001): 23-30.

Wang, Jianxin and David B. Wolff. “Evaluation of TRMM Ground-Validation Radar-Rain Errors Using Rain Gauge Measurements.” *Journal of Applied Meteorology and Climatology* 49.2 (2010): 310-324.

Willmott, C.J. “On the Validation of Models”. *Physical Geography* 2 (1981): 184-194.

Willmott, C.J. and Kenji Matsuura. "Advantages of the mean absolute error (MAE) over the root mean square error (RMSE) in assessing average model performance." *Climate Research* 30.1 (2005): 79.

Yamamoto, Ken’ichi and Kenjii Kakamura. “Comparison of Satellite Precipitation Products with Rain Gauge Data for the Khumb Region, Nepal Himalayas.” *Journal of the Meteorological Society of Japan* 89 (2011): 597-610.

Yang, Daqing, et al. "Accuracy of NWS 8 standard non-recording precipitation gauge: Results and application of WMO intercomparison." *Journal of Atmospheric and Oceanic Technology* 15.1 (1998): 54-68.

Zhou, T et al. “Summer precipitation frequency, intensity, and diurnal cycle over China: a comparison of satellite data with rain gauge observations.” *Journal of Climatology* 21 (2008):3997–4040